IEEE Access
Multidisciplinary | Rapid Review | Open Access Journal

Received 11 November 2022, accepted 24 November 2022, date of publication 28 November 2022,
date of current version 5 December 2022.

Digital Object Identifier 10.1109/ACCESS.2022.3225119

TOPICAL REVIEW

A Review of Modeling and Mitigation Techniques for Bearing Currents in Electrical Machines With Variable-Frequency Drives

WENJUN ZHU[1], (Graduate Student Member, IEEE), DANIELE DE GAETANO[1], (Member, IEEE), XIAO CHEN[1], (Senior Member, IEEE), GERAINT WYN JEWELL[1], AND YIHUA HU[2], (Senior Member, IEEE)

[1]Department of Electronic and Electrical Engineering, University of Sheffield, S10 4DE Sheffield, U.K.
[2]Department of Electronics Engineering, University of York, YO10 5DD York, U.K.

Corresponding author: Xiao Chen (xiao.chen@sheffield.ac.uk)

This work was supported by the U.K. Engineering and Physical Sciences Research Council (EPSRC) under Research Award EP/W015838/1.

ABSTRACT The converter switching in variable-frequency drives can generate high frequency common mode voltage between the machine winding and the converter ground, leading to high frequency parasitic currents which can flow through the machine bearings unless precautions are taken in design and installation. These parasitic and unintended currents in the bearings cause deterioration of the lubrication film and surface damage to the rolling elements of the bearings. These problems will be exacerbated as wide-bandgap semiconductors with faster switching rise times start becoming more widespread in variable-frequency drives. This paper reviews the modelling and mitigation techniques of high frequency bearing currents in inverter fed AC drives. It aims to provide a solid base for the research community to further understanding the bearing currents phenomenon and helping to find novel improved technique for their mitigation and measurement.

INDEX TERMS AC machines, bearing current, common mode current, common mode voltage, variable frequency drives.

I. INTRODUCTION

In 1920s, bearing current were observed with coking of the oil, pitting of the bearing and scoring of the shaft [1]. At that time, which predated the emergence of modern power electronics, most AC machine were fed directly from sinusoidal line voltage. It is recognized that the magnetic field asymmetries, aligned with the machine shaft, induce voltage in it during operation, generating the ''shaft voltage''. The asymmetries are inherently caused by the manufacturing displacement of the machine even within the tolerances. Additional causes of these asymmetries are the anisotropy of magnet's remanence and permeability of iron core materials. Shaft voltage and bearing current fed by sine wave are somehow with the orders of the fundamental frequency. Low frequency bearing currents are not the focus of this paper, hence they will not be discussed in detail.

From the 1970s onwards, variable frequency drives (VFDs) have been deployed increasingly across many industry sectors. due to their advantages of flexibility, efficiency and high performance in torque and speed control. A growing proportion of AC machines, mainly induction machines (IMs) and permeant magnet synchronous machines (PMSMs), are now inverter-fed across a wide range of power levels. The typical switching frequency values of power electronic devices (IGBT, MOSFET, etc.) controlled using pulse width modulation (PWM) techniques, are several kHz up to tens of kHz. The high switching frequency generates a high frequency common mode voltage (CMV), which subsequently results in shaft voltage which can in turn give rise to a bearing current through the capacitive and inductive coupled paths in the AC machine.

The associate editor coordinating the review of this manuscript and approving it for publication was Giambattista Gruosso.

Once the bearing current density exceeds a particular threshold, the metallic structure and lubricants of the bearings could be progressively damaged, hence significantly curtailing bearing life. According to the surveys in [1], around 30 percent of all motor failures are resulted from electrical bearing damage. A questionnaires-based survey of the bearing failures with 3934 samples of sinusoidal drive and 286 samples of variable speed drive showed that the drives fed by converters are 12 times more likely to exhibit bearing failures than the drives fed by line voltage [2]. Hence, additional attention should be paid to the bearing currents in machines fed by PWM inverters.

Nowadays, the emerging device technologies of SiC and GaN has allowed significant increases in switching frequency and given rise to dramatic increases in dv/dt. Whereas the high switching frequencies and lower switching loss capability of SiC and GaN provide a route to more compact and power dense inverters, the increases in dv/dt exacerbates the stress on the bearings.

Many studies have been carried out to understand the underlying mechanisms involved in bearing currents and corresponding mitigation methods. Four types of current damage on bearings are reviewed in [3], viz. frosting, spark tracks, pitting and welding. Actual field cases and solutions are reviewed in [4] but without detailed theoretical and quantitative analysis. A top-level introduction to bearing currents is presented in [5] and mainly focuses on presenting commercial, and straightforward techniques for mitigation of bearing current in classic PWM inverter drives, e.g. inverter output filters and insulated bearings. Methods requiring special hardware or motor modifications are not discussed. An evaluation of mitigation techniques for bearing currents, electromagnetic interference (EMI) and over-voltages in adjustable speed drive applications is carried out in [6]. It serves as a useful reference tool for to perform the necessary measurements and then determine if there is a potential VFD-related problem. If a problem is detected, one of the suggested mitigation techniques can be applied. These mitigation techniques include, inter-alia, shaft grounding system, insulated bearings and journals, ceramic bearings, conducting grease, a Faraday shield, and a new dual-bridge inverter designed to eliminate the common mode voltage. An overview of various modelling techniques for an AC machine and inverter system, specifically for the mid- and high-frequency ranges, is described in [7]. However, these models are mainly developed for EMI analysis and hance have limited read-across the bearing currents because the frequency of EMI phenomenon is in the range of several to tens of MHz, which are higher than the frequency of bearing currents. The mechanism and mitigation techniques of shaft voltages and bearing currents in electric vehicle and hybrid electric vehicle motors are reviewed in [8]. An overview of the techniques for monitoring the state of bearings as well as low frequency conventional and high frequency inverter generated shaft voltages is presented in [9]. However, neither [8] no [9] report on any thorough modelling or computation.

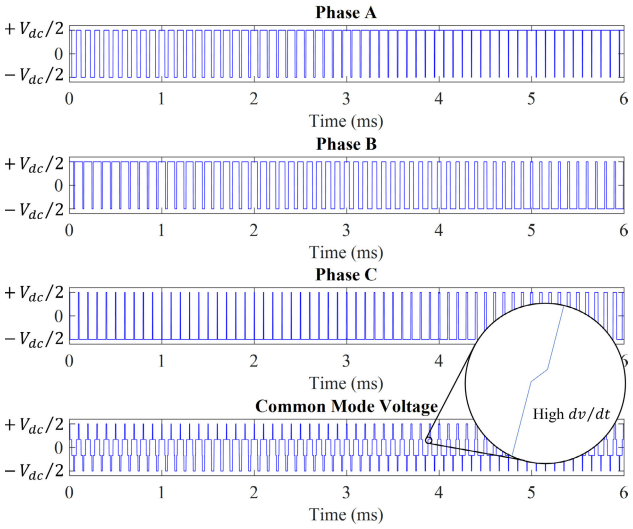

FIGURE 1. Example of PWM Inverter Output Phase Voltages and Common Mode Voltage.

In existing literature, there is arguably a lack of a systematic in-depth review on bearing currents in inverter driven machines which encompasses the underlying physical mechanisms, modelling, prediction and mitigation strategies and associated technologies. This paper aims to review these inter-linked aspects of research on bearing currents with a view to providing a comprehensive review of beating current phenomena.

II. PHYSICS OF BEARING CURRENTS

A. COMMON MODE VOLTAGE

In this section, the classic configuration of a 3-phase full bridge PWM inverter is used as an example to demonstrate the mechanism by which common mode voltages are produced. The output voltage of each phase is switched between $+V_{dc}/2$ and $-V_{dc}/2$. In a star-connected machine, the neutral to ground voltage is the zero-sequence voltage, expressed in (1).

$$V_{com} = \frac{V_A + V_B + V_C}{3} \tag{1}$$

The frequency of the common mode voltage is 3 times the switching frequency and the switching action produces very high dv/dt, typically up to $10kV/\mu s$, as shown in Fig. 1. The works [10], [11] have demonstrated that the common mode voltages generated by a PWM technique, in an inverter-motor system, couple through parasitic capacitances from stator windings to the rotor body and then return through the motor bearings to the grounded stator case as a closed loop circuit. This common mode voltage has been considered as the source of the bearing currents in inverter-motor systems.

The experimental study reported in [12] demonstrates that the RMS value of common mode voltage increases with an increase of switching frequency and a decrease of motor speed. However, the peak magnitude is affected by switching frequency only.

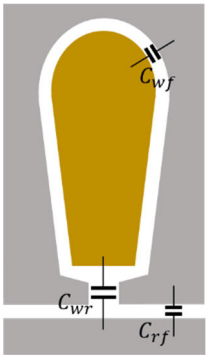

FIGURE 2. Parasitic capacitances in an AC machine.

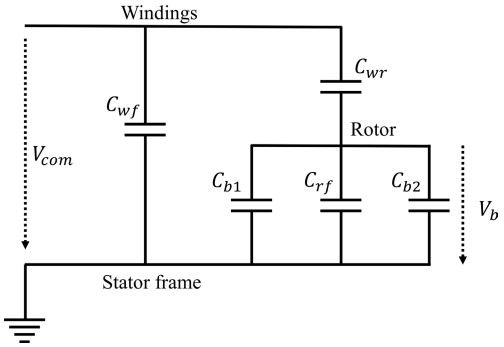

FIGURE 3. The common mode capacitive coupling circuit.

Medium-voltage inverters (i.e. operating from DC links of 1kV and upwards) usually employ different power converter topologies and switching strategies compared low-voltage converter, but they still generate common-mode voltages and currents which can cause a very high dv/dt [13]. The common mode voltage of the following 5 different PWM methods are compared in [14] in terms of the frequency, magnitude, modulations index, control index, voltage distortion factor, etc.: the fully controlled operation (FCO), the classical space vector modulation (SVM), the three active vector modulation (3AVM), the two additional space vectors (AZVC-2) and the one additional inverse voltage vector (AZVC-1). Since the common mode voltage is the fundamental source of bearing currents, considerable research efforts have been directed towards the reduction of the common mode voltage from the source. Proposed solutions are mainly focused on new topologies and new modulation technologies such as multi-level inverters and dual-bridge inverters.

B. FOUR TYPES OF BEARING CURRENT MECHANISMS

Traditional AC machine models tend to neglect high frequency phenomena. However, in the high frequency domain, which in the context of electrical machines corresponds to frequencies of tens of kHz or higher, the stray capacitances or parasitic capacitances in the machine provide a path for the bearing current between two conducting region which are separated by an insulating layer of material conductors naturally form a capacitor. In the conventional 3-node lumped parameter model, the main parasitic capacitances in the machine have been identified as winding-stator frame capacitor C_{wf}, winding-rotor capacitor C_{wr}, and stator-rotor capacitor C_{rf}, as shown schematically in one stator slot in Fig. 2. An example of the equivalent circuit model was built based on the machine structure as shown in Fig. 3.

Muetze, Binder et al. have published numerous papers [15], [32] on systematic research into bearing currents in IMs. They noted that bearing currents can be classified into four types based on their different mechanisms [15].

1) CAPACITIVE BEARING CURRENTS

The common mode voltage has a divider V_b across the bearings when the lubricant film formed in operation and the bearings act as capacitors, C_{b1} and C_{b2}.

The bearing voltage ratio (BVR), which is a key indicator of the bearing voltage, is defined in (2).

$$BVR = \frac{V_b}{V_{com}} = \frac{C_{wr}}{C_{wr}+C_{rf}+2C_b} (\text{assume } C_{b1} = C_{b2} = C_b) \tag{2}$$

The resulting capacitive bearing current can be calculated by (3).

$$i_b = C_b \frac{dv_b}{dt} \tag{3}$$

If the speed is low ($< 100rpm$), the bearing ball may contact the races and hence the bearing is equivalent to a resistor. The amplitude of this bearing current is typically $\leq 200mA$.

2) ELECTRIC DISCHARGE MACHINING (EDM) CURRENTS-i_{EDM}

If the v_b is high enough to cause electrical breakdown of the lubricant film, the energy stored in the rotor-frame capacitance discharges and generates an impulse current. The dielectric lubricant can flow into the channel and form a new insulation film, and thus the bearing capacitance charges again. This breakdown-recovery-breakdown process repeatedly continues. The so called EDM current damages the bearing with each impulse as the discharged energy damages the metal surface. This process progressively increases the presence of metallic particles in the lubricant, which exacerbates on-going electrical breakdown. The vicious circle accelerates bearing failure.

3) CIRCULATING BEARING CURRENTS-i_{CB}

The circulating bearing currents were first described by S. Chen et al. in [33] and [34]. The common mode voltage generates a high frequency common mode current which flows in the winding→stator→ground path. This high frequency current induces a common mode flux which further generates a high frequency voltage along the shaft. The shaft voltage causes the circulating bearing currents in the loop: shaft → driving end bearing→stator frame→non driving end bearing→shaft.

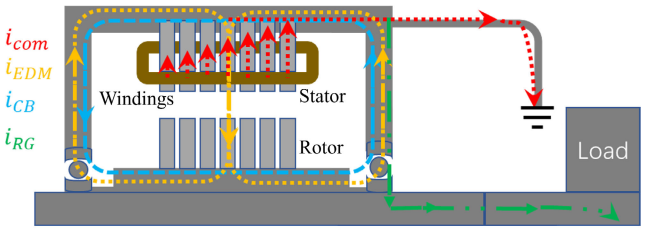

FIGURE 4. Bearing current loops.

4) ROTOR GROUND CURRENTS-i_{RG}

The rotor can be grounded via load in some cases. If the impedance of rotor to ground is much lower than the stator to ground impedance, a proportion of the ground current will flow from the rotor through the bearing, since the current flows predominantly in the path with the lowest impedance. This type of current is noted as rotor ground current.

Since the capacitive bearing currents are usually too small to be harmful to the bearings, in some literature only the last 3 types of bearing currents are recognized [35], [36]. Fig. 4 shows schematic current flow loops of the common mode current i_{com} and the other 3 types of bearing currents.

The rotor ground current should be investigated on a case-by-case basis as it is only present if the rotor is grounded, meaning it depends on the configuration of the load. The different load configurations are generally regarded out of scope of the ''inverter-cable-machine'' system modelling. Hence, the main interest in published studies has been on the modelling and prediction of the EDM and circulating currents.

In order to fully analyze bearing currents, a closed system modelling is needed, which includes inverter, cables, and an appropriate fidelity model of the machine. In some applications, the cables which connect the inverter to the machine could be tens of meters long. The impedance of these cables, including the grounding impedance, directly affects the common mode current $\boldsymbol{i_{cm}}$, and eventually influence the nature and magnitude of the bearing currents. Second order RLC-circuits, ladder-circuits and/or transmission-line representations are used to model the cables with due account the wave propagation phenomena. Some research on the EMI of electrical machines have put considerable effort into modelling the cables in the HF domain [37], [39]. These various studies also contribute to the understanding of bearing currents, in which only with the cable model is an important element in determining the overall system level behavior.

III. CAPACITIVE EDM CURRENT

The generic theoretical bearing current mechanisms fed by PWM inverters have been described in the previous sections. However, the lumped parameter circuit models require significant in-depth analysis to establish representative values of the circuit parameters which reflect the complex geometry and material composition of a typical electrical machine.

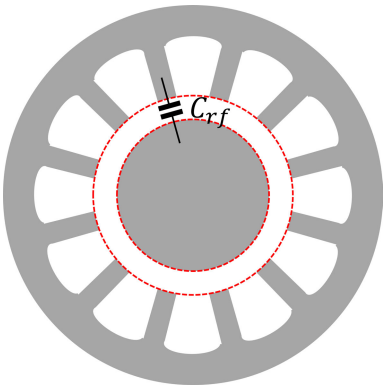

FIGURE 5. Illustration diagram of rotor-to-frame capacitance C_{rf}.

A. MODELING BASED ON THE MEASUREMENTS

For the purpose of extracting the circuit parameters, magnitude and phase of the impedance between the windings, the stator frame and the rotor were extracted from the measurements with signal generator excitations, often using an impedance analyzer. The measured output waveforms are used as a reference for calibrating the response of LCR circuit models [40], [41]. Indeed, in contrast to analytical methods based on representations of the physics of the actual geometry, measurement based methods treats the parasitic parameters as something of a black-box, and the equivalent circuit model and component values are formulated to match the measured responses.

A universal high-frequency lumped-parameter model which can represent the delta-connected IMs was proposed in [42]. The parameters were calculated by an iterative method to match the measured common and differential-mode impedance curve. Based on this model, the EDM current and common mode current can be predicted. Similar approaches were employed by [43], [44], [45], and [46], despite different complexity and data fitting algorithms, e.g. the trial-and-error method [43], the least-squares data fitting [44], the vector fitting technique [45] and the genetic algorithm [46].

B. ANALYTICAL MODELING

The use of measurement to characterize a particular machine is not the only method that can be used identify the capacitance parameters. They can be analytically and straightforwardly calculated by simplifying the machine geometry and drawing on well-established formulae for the capacitive of different electrode configuration. The plain plate and the cylinder model of capacitors are commonly used to calculate the rotor-to-frame capacitance C_{rf}, the winding-to-frame capacitance C_{wf}, and the winding-to-rotor capacitance C_{wr}.

The rotor-to-frame capacitance C_{rf} (Fig. 5) is considered as a cylinder capacitor with a Carter coefficient k_c used to correct the opening slot effects. It has been shown that neglecting the cage rings can result in a 15%-30% underestimate of C_{rf} in squirrel cage IMs [22].

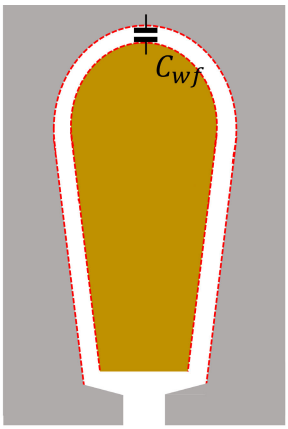

FIGURE 6. Illustration diagram of winding-to-frame capacitance C_{wf}.

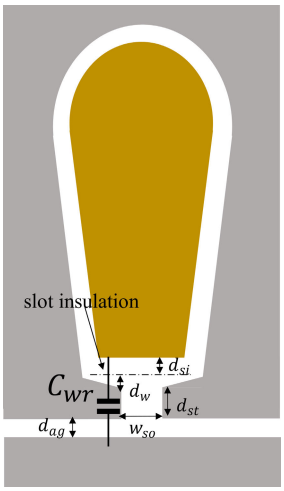

FIGURE 7. Illustration diagram of winding-to-rotor capacitance C_{wr}.

The winding-to-frame capacitance C_{wf} (Fig. 6) can be calculated by adopting an approximation to a plain parallel plate capacitor. The area of the electrodes is the circumference of stator slot multiplied by the axial length of stator lamination stack.

The winding-to-rotor capacitance C_{wr} (Fig. 7) is modelled as Q_s plate capacitors in parallel, where Q_s is the number of slots. Again, each parallel plate capacitor is modelled as several capacitors in series, such as the capacitance of the air gap, the slot, the slot wedge, and the upper slot insulation. In Fig. 7, d_{ag} is the air gap length, w_{so} is the slot opening width, d_{st} is the height of the teeth tip, d_w is the height of the wedge, and d_{si} is the height of the insulation layer.

Due to its simplicity and direct physical link to known dimensions, such simplified analytical methods are widely used to calculate the parasitic capacitances for both IMs and PMSMs [15], [23], [47], [59].

However, the aforementioned analytical methods treat the complex stranded windings as a single node. Hence, it cannot capture the unequal sharing of voltage between various turns in one winding coil, resulting in errors in the predictions of common mode current, shaft voltage and bearing current. Furthermore, the end-winding effect is usually neglected in such simplified analytical methods, which can underestimate the winding-rotor capacitance C_{wr} by ∼90% as reported in [60].

C. 2D FINITE ELEMENT MODELING

To account for the stranded coil effect, researchers have employed electrostatic finite element methods (FEM) to perform detailed electrical field calculations and so extract values of machine capacitances. The mutual capacitances of multi-conductor system can be considered by the capacitance matrix method. Considering the stator-frame, the windings, the rotor as 3 nodes in the machine, the relationship between the voltage of windings V_w, the voltage of rotor V_r, the voltage of stator V_s, the electric charge of windings Q_w, the electric charge of rotor Q_r, the electric charge of stator Q_s can be expressed as:

$$\begin{bmatrix} Q_w \\ Q_r \\ Q_s \end{bmatrix} = \begin{bmatrix} C_{wf}+C_{wr}+C_{rf} & -C_{wr} & -C_{wf} \\ -C_{wr} & C_{wf}+C_{wr}+C_{rf} & -C_{rf} \\ -C_{wf} & -C_{rf} & C_{wf}+C_{wr}+C_{rf} \end{bmatrix} \times \begin{bmatrix} V_w \\ V_r \\ V_s \end{bmatrix} \quad (4)$$

In [61], 2D FEM was used to calculate the capacitance, comparing the results with the analytical method. The comparison showed that there is a large difference between the methods in the calculation of the winding to magnet capacitance in a PMSM. This can be explained as the simplified model neglects the edge effects in which flat or cylindrical based capacitances cannot take such phenomena into consideration. A 2D FEM, which considers a double-layer winding wound from rectangular wires insulated with Kapton CR tape insulation, was investigated in [62] for a traction induction machine. The capacitance results were shown to be in accordance with measured values. Additional 2D FEM approaches to capacitance calculations can be found in [62] and [66].

The overall stray capacitance C_{wf} is considered to be composed from a number of distributed (turn-to-turn C_{tt} and turn-to-core C_{tc}) capacitances connected in series-parallel combination [62]. The turn-to-turn detailed coil model is illustrated in Fig. 8 (a) whereas the random wound coil is illustrated in Fig. 8 (b).

D. 3D FINITE ELEMENT MODELING

One straightforward method to account the end-winding effects is to use 3D model. A 3D FEM model of an induction machine with end-windings (shown in Fig. 9) was constructed in [67], for the purposes of comparing the 2D and 3D models without end windings. In [60], 3D FEM models were built with end-windings to investigate the electrostatic shielding effects and compare the winding-rotor capacitances of models with and without end-windings. The results showed that the end-windings have significant effects on

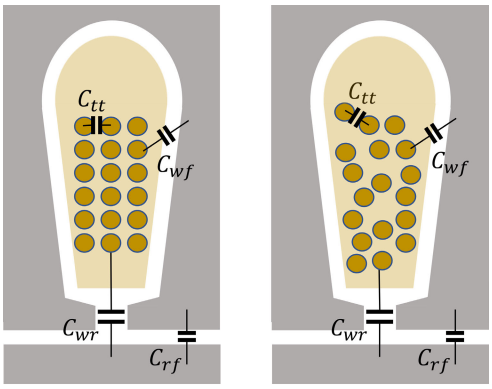

FIGURE 8. 2D slot model of uniform wound coil (a) and random wound coil (b).

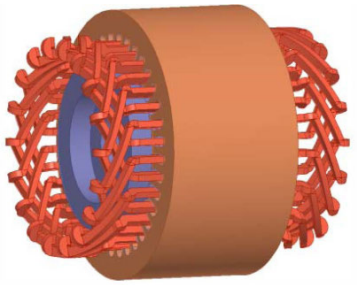

FIGURE 9. 3D model with the end windings [67].

the winding-to-rotor capacitance, and neglecting their contribution can underestimate the winding-rotor capacitance by 40%-90%.

3D FEM analysis has also applied to salient pole synchronous machine in [68], taking into consideration the end-winding effect The parameters of capacitances, extracted from the 3D FEM model, were fed into the equivalent circuit model. The calculated common mode impedance curve matches the measured values over a wide frequency range [69].

Additionally, it is also possible to include the influence of the rotor end-plate into the 3D model. Hence, the rotor-to-plate capacitance can be analyzed. A comparison of merits and drawbacks of different parameter identification methods for parasitic capacitances in electrical machines is summarized in TABLE 1.

The calculated or measured capacitances can be incorporated into the common mode circuit (Fig. 3). When used in combination with a bearing circuit model, the EDM current can be predicted.

IV. INDUCTIVE CIRCULATING BEARING CURRENT

The circulating bearing current i_{CB} whose path was shown schematically in Fig. 4 is generated by the induced shaft voltage which results from the common mode current i_{com}. The circulating bearing current and the common mode current are coupled via the common mode flux. The mechanism can be considered as a transformer with the primary side having common mode current and the secondary side with

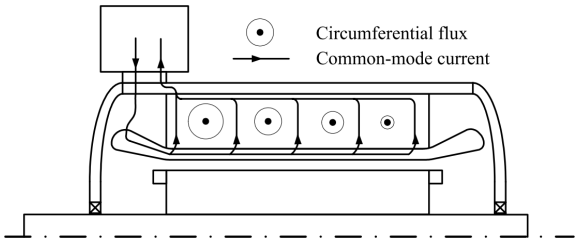

FIGURE 10. The path of the common-mode current and the distribution of the circumferential high-frequency common-mode magnetic flux encircling the shaft. The magnitude of the flux is illustrated by the size of the circles [36].

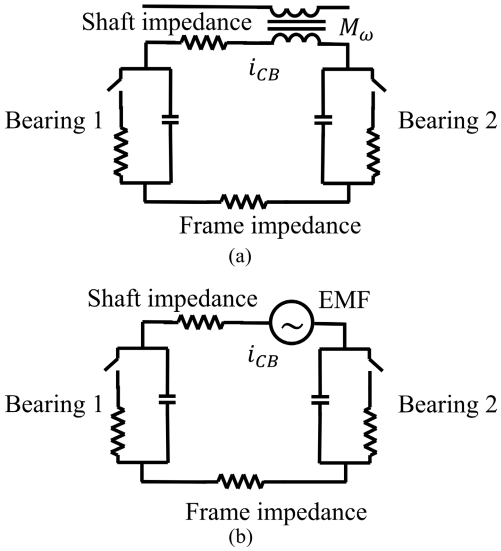

FIGURE 11. Equivalent circuit of circulating bearing current (a) with mutual inductance; (b) with EMF source.

circulating bearing current. Fig. 10 shows the path of common mode current and the distribution of circumferential flux [36].

A. CIRCUIT MODEL OF CIRCULATING BEARING CURRENT

Due to skin effect, the high frequency circulating current follows a zigzag path in the stator laminated core. One equivalent circuit model which can be used to represent this behavior is a frequency dependent mutual inductance M_ω or a current controlled voltage source [56], which are key elements for modelling the circulating bearing current and the shaft voltage, as shown in Fig. 11.

The common mode voltage generates the common mode current which flows via the winding-to-stator capacitor into the stator laminations. The impedance of the stator core is strongly frequency-dependent due to the skin effect. The skin and proximity effects are taken into account by modeling the resistances and inductances by ladder circuits such as those shown in Fig. 12 [70]. Typically, 3-4 orders of ladder circuits are used to represent the measured impedance curve with a wide frequency band.

B. ANALYTICAL CALCULATION OF i_{CB}

In a similar manner to the parasitic capacitance, analytical methods can be applied to calculate the impedance of the circulating current loop based on a few simplified assumptions.

TABLE 1. Comparison of Various Parameter Identification for Machine Capacitances.

Methods	Merits	Drawbacks
Impedance measurement & fitting algorithm	-Reliable and can be used to validate other methods -No assumption and naturally take all the factors into account	-Limited inspection points and difficult to decouple specific capacitances from adjacent capacitances (such as the decoupling difficult in turn-turn capacitances) -Cannot be performed in the design phase
Analytical methods based on simplified geometrical representations	-Computationally efficient -Convenient for the initial capacitance estimation	-Very reliant on generic approximations -Difficult to accurately quantify the end-winding effects and turn-to-turn capacitances
2D FEM	-Turn-to-turn capacitances can be considered in 2D plane model -Simplified representation of end-winding effects can be considered in axisymmetric models	-Neglects turn-to-turn capacitance in axisymmetric models -Neglects end-winding effect in 2D plane models
3D FEM	-High accuracy if all the essential components are modelled with accurate properties and positions -Capable of accounting for the 3D end-winding effect and turn-to-turn capacitances simultaneously	-Onerous computation load -Detailed geometry and material information required

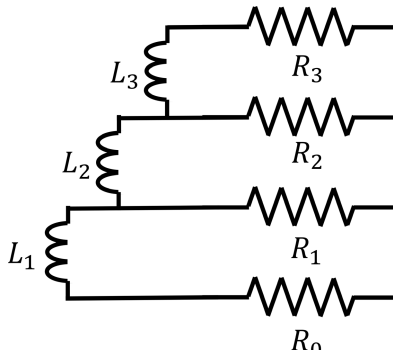

FIGURE 12. Ladder circuits for modelling the skin effects.

An approach to common mode circumferential flux calculation is presented in [71] and [72]. Based on the common mode circumferential flux, an analytical calculation of the mutual inductance and the resulting circulating current path impedance was reported in [22]. This study noted that the calculated maximum bearing current ratio (BCR), which the ratio of the circulating bearing to common mode current, is approximately 0.35.

In this study reported in [22], the analytical calculation of circumferential flux and induced voltage can be performed using:

$$\phi_0 = \mu \frac{N_{Fe} i_{com}}{2\pi} \ln\left(\frac{d_{se}/2}{d_{si}/2 + h_s}\right) \frac{\delta_s}{\sqrt{2}} \tag{5}$$

$$v_{max} = 2\pi f \phi_0 = \mu_0 \mu_r N_{Fe} \hat{i}_{com} f \ln\left(\frac{d_{se}/2}{d_{si}/2 + h_s}\right) \frac{\delta_s}{\sqrt{2}} \tag{6}$$

where N_{Fe} is the number of sheets of stator core, d_{se} is the outer diameters of stator lamination, d_{si} is the inner diameters of stator lamination, h_s is the height of stator slot, δ_s is the skin depth and f is the frequency of common mode current. These analytical formulas are derived based on the assumption that the common mode current flows into each stator lamination sheet equally, denote as i_{sheet}, and flows into the neighboring sheet through a zig-zag path in the surface of laminations, due to skin effects, until the very last sheet as shown in Fig. 13.

The analytical method and the measured data fitting were combined to develop a 3 phase IM model to analyze the capacitive and inductive shaft voltage simultaneously in [73].

C. FINITE ELEMENT CALCULATION OF i_{CB}

The investigation reported in [63] analyzed the resistances and inductances based on a FEM eddy current model which proposed a high frequency lumped model for PMSM. The parameters were extracted by using a 2D FEM model. The resistance and inductance of each individual winding turn were calculated by time harmonic finite element analysis. The self-capacitance of each turn and the mutual capacitances between turns were evaluated by electrostatic FEM calculations. The distributed parameter winding circuit was reduced to a π model branch by Kron reduction technique.

In a study reported in [74] the common mode flux was calculated by 2D axisymmetric FEM and combined with an analytical method. It was demonstrated that the rotor impedance cannot be neglected at high frequency as it is often comparable to the stator impedance. Moreover, it was shown

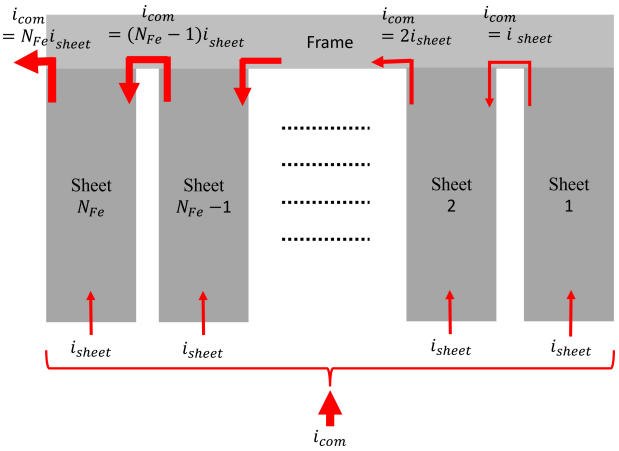

FIGURE 13. Common mode current path of the lamination sheets.

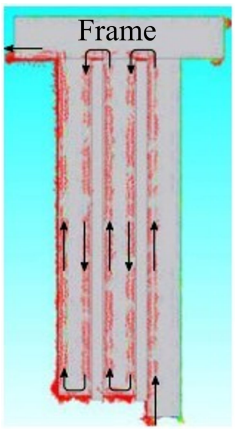

FIGURE 14. FEM predicted current density distribution of the common mode current flow from the rightmost sheet to the left end of the frame [69].

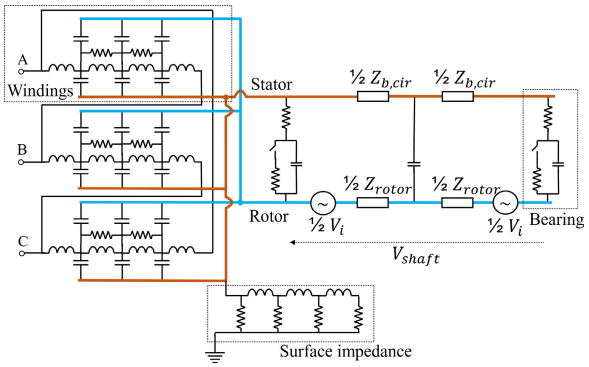

FIGURE 15. Complete model for capacitive and inductive bearing current [69].

that the circulating bearing currents can be mitigated if the rotor impedance is significantly increased.

An elaborate 3D model of the induction motor in [75] takes into account the nonlinear B-H characteristics of ferromagnetic cores, skin effect in cage bars, magnetic field space harmonics, rotational motion of the rotor as well as the anisotropy of the laminations.

A full-3D FEM field analysis including inductive and capacitive couplings would be too demanding in terms of computational resources. It also presents stability problems as the frequency range of interest varies from a few Hz to MHz. To avoid these difficulties, a 10° section of the PMSM was modeled in 3D FEM in [76]. The mutual inductance M_ω, and the circulating bearing-current loop inductance were obtained by solving the 3D magnetic stationary current distribution boundary value problem.

Once the induced flux and impedance of the laminations are calculated, the circulating bearing currents can be predicted.

V. COMBINED EDM AND CIRCULATING CURRENT MODELING

Distinguishing between different mechanisms and contributions to the overall bearing currents helps to understand their individual cause-and-effect chains, which in turn provides insight into effective mitigation methods. However, such a superposition approach with separate modelling of EDM current or circulating currents may lead to an underestimation of total bearing currents due to the fact that the bearings could be in a deeper breakdown condition with a smaller resistance under the two types of bearing currents than only one type of bearing currents modelled. A combined model which can predict the EDM and circulating currents simultaneously is necessary to evaluate the risk of bearing damage.

Relatively few published studies have quantified the two bearing current components simultaneously.

A comprehensive high frequency model of an induction machine was proposed in [69], employing parasitic capacitances derived from 3D FEM. The stator core impedance is derived from a 3D FEM model of the eddy current distribution in a representative model based on three laminations. A measured impedance curve fitting approach was used to identify the remaining parameters. The current path of 3D FEM model, which is shown in Fig. 14, matches with the assumption made in the analytical method (Fig. 13). Then the ladder circuit is used to represent the frequency-dependent impedance, shown as the "surface impedance" in Fig. 15, to complete the circuit model of EDM and circulating current.

Fig. 16 shows a lumped parameter circuit model proposed in [76] in which the paths of i_{com}, i_{EDM} and i_{CB} are clearly identified, and the parameters are derived by FEM.

The basic idea of the combined EDM and circulating bearing currents modelling is to connect the two different current paths into one complete circuit model. The capacitance of the circuit would be mainly geometry dependent, and the resistance and inductance depend on frequency (due to skin effects) and permeability (due to saturation of soft magnetic materials).

VI. MODELING OF A ROLLING ELEMENT BEARING

The bearing itself exhibits a complex nonlinear electrical impedance. The load, speed of revolution, temperature and lubricant conditions all affect the impendence of a rolling element bearing [77]. To predict the magnitude of the bearing currents, a detailed electrical bearing model is essential.

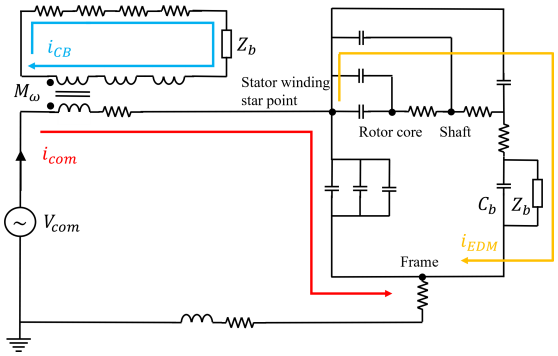

FIGURE 16. Equivalent lumped parameter model [76].

A. BREAKDOWN OF BEARINGS AND EQUIVALENT CIRCUIT MODEL

When stationary or rotating at low speed, the balls or rollers make metallic contact with the races and the impedance is predominantly resistive. With the shaft speed increasing, the bearing lubricant creates a dielectric oil film between balls and raceways. The thickness of the lubricant film, which is highly dependent on the viscosity, can be estimated by hydrodynamic theory. In this condition, the bearing acts essentially as a capacitor.

If the bearing voltage exceeds a certain threshold value, the electrical field strength is sufficient to generate a discharge path in the lubricating oil film between the metallic balls and the inner/outer races. This process results in electrical breakdown of bearings. During the process of breakdown, the bearing impedance changes its behavior from a predominantly capacitive state to being predominantly resistive. The typical threshold electric field strength is approximately 15 V/μ m [49]. Considering that in most beating the lubricant film thickness ranges from $0.1 - 2\mu$ m, the reference breakdown voltage is therefore typically in the range $1.5 - 30$V.

It is well known that the breakdown voltage varies with the machine speed. Increasing the shaft speed tends to increase the oil film thickness and hence on the one hand it become more difficult to initiate breakdown for a particular bearing voltage. However, at the same time, residual metallic particles in the lubricants pass the breakdown channel more frequently, allowing the discharge to happen more readily at a particular voltage. These two counteracting effects result in a more nuanced, and application specific, variation in breakdown voltage with speed variation.

Several different bearing equivalent circuit models have been proposed in literature, albeit they share many of the same principles and approaches. Bearings are commonly represented as a capacitor and resistors in a parallel/series arrangement with a switch to represent the breakdown or non-breakdown state. Fig. 17 illustrates four examples of bearing equivalent circuit presented in literature.

B. ANALYTICAL MODELING OF BEARINGS

Busse et al. [49] proposed an analytical method for a-priori parameters estimation for a given bearing design. The model

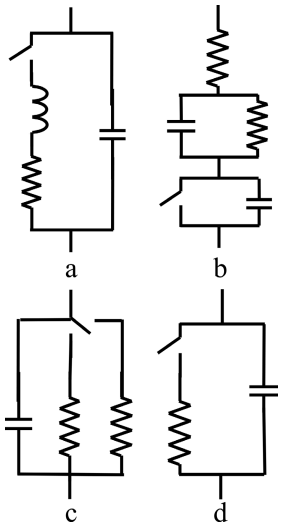

FIGURE 17. Impendence models for a rolling element bearing (a[11];b[77], [78];c[79];d[80]).

employed for ball bearings assumes several pairs of concentric spheres. Each capacitor pair includes an inner sphere (representing the balls) within an outer sphere (modeling the raceways). Furthermore, a theory of Hertzian contact area from [48] was drawn on in order to model the capacitance of bearings. The Hertzian contact area A_{H} is taken as the corresponding electrode area [23]. This method is now widely accepted as an effective and convenient, is rather simplified, model for bearing capacitance.

Gemeinder et al. [79] developed an electrical bearing model based on detailed mechanical calculations for radial ball bearings. The bearing load, contact area and lubrication film thickness were taken into the consideration. The model demonstrates a good fit between the measured and calculated impedance in the frequency range from 10 kHz to 10 MHz. However, for frequencies outside this range, there were notable discrepancies between the model and measurements.

C. FEM MODELING OF BEARINGS

In addition to the analytical method, FEM has also been applied to bearing modelling. Jun et al. [81] modelled a bearing equipped with 14 rollers using 2D FEM. Each roller was considered as being electrically in parallel with the remaining rollers. The capacitance between outer race and roller (C_{bo}) and the capacitance between inner race and roller (C_{bi}) are series connected. The capacitance between outer race and inner race (C_o) is in parallel to the branch of C_{bo} and C_{bi}, as shown in Fig. 18.

The influence of gravity and/or an applied load can give rise to both an asymmetric ball position and an asymmetric shaft position, especially at low speeds. A 2D FEM analysis for extracting the bearing capacitance was performed in [82]. The bearing capacitance is not constant but has a nonlinear relationship with load and speed. 3D electrostatic field solver analysis was implemented by Cay et al. [83], where they calculated the bearing capacitance in pre-breakdown state.

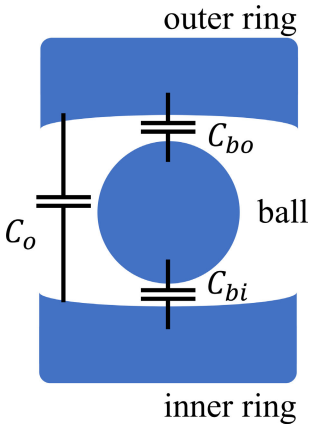

FIGURE 18. Per ball model of bearing.

D. EXPERIMENTAL TESTS

Prashad [84] carried out an experimental study on bearing discharge with different operating parameters. It focused on the threshold voltages and impedance response of non-insulated rolling element bearings under the influence of various levels of electrical currents. However, the test was undertaken with a low frequency source rather than a high frequency switching source.

During operation, the capacitances of the inner/outer raceway and balls are not constant but vary with the motor shaft speed and load. Zhu et al. [85] described the effect of load distribution (viz. gravity, unilateral magnetic pull and centrifugal force) and speed on the contact area and oil film thickness between each rolling element and the raceways and concluded that the speed has a marked influence on the film thickness.

Krzemien [86] performed an investigation of the electrical properties of ball bearings by testing the discharge current pulse number per revolution in DC, low frequency AC and high frequency AC bearing voltages. The test results showed that the increase in bearing voltage values causes the value of the bearing critical temperature (at which the bearing current pulse number per shaft revolution reaches its maximum) to decrease.

In contrast to the conventional constant resistance model which is commonly used to represent the breakdown state, a variable resistance model of bearings was proposed by Ren et al. [87]. It suggested that the breakdown process can be divided into 3 intervals: the starting interval, the stable interval, and the recovery interval. The resistance was described as 3 different time dependent values according to the arc discharge model principle.

A statistical approach was applied in [88] to study the EDM current since it appears intermittently and seems to depend on many complex factors such as a level of shaft voltage, motor speed and temperature. It was observed that the EDM currents occur within a reasonably steady window of shaft voltage, even though most of events occur at the higher levels of shaft voltage [89]. It was reported in [90] that the incidences of EDM current pulses are not necessarily synchronized with the edges of the common mode voltage. This phenomenon cannot be explained straightforwardly by the classical equivalent bearing model which is based on a comparison between the instantaneous bearing voltage and the fixed value of threshold breakdown voltage. However, it is recognized that this approach has a shortcoming in that the threshold breakdown voltage varies during operation. Hence, if the switch in the model can be activated by the energy stored in the lubricant instead of by the threshold voltage, the prediction of EDM current can be improved [80].

A statistical or enhanced model which considers the influence of the operating conditions, viz. shaft speed, temperature, load, lubricant decomposition, etc. on the bearing breakdown could provide the basis for improved switch control in the model for an improved EDM current prediction.

VII. MITIGATION METHODS

By using physically based models, it is possible to calculate the bearing current magnitude and hence devise and analyze the effectiveness of different mitigation methods within a drive system. At the system level, mitigation methods can be applied on the motor side, the inverter side, and on the connections. Schiferl et al. [91] summarized 7 different mitigation options which can be applied on the motor side. It was noted that effective remediation methods depend upon a thorough understanding of the potential current paths in each installation. Bjekic et al. [5] reviewed the mitigation methods applicable to existing installations with the straightforward addition of equipment. The influence of the cable type was discussed in [17] which also summarized different mitigation techniques such as filters, insulated bearings, and hybrid bearings on the bearing current phenomena for machines at 11 kW to 500 kW power levels.

A. MITIGATION WITHIN THE INVERTER

In order to reduce the bearing current from the source, mitigation methods can be used on the inverter side. These can include new modulation technologies, new topologies, or a combination thereof, with the aim of reducing the amplitude and/or dv/dt of the common mode voltage.

A simple PWM scheme which alleviates the common mode voltage problems in three level inverter applications was proposed in [92]. Zhao et al. [93] proposed a hybrid selective harmonic elimination pulse width modulation scheme to reduce the common-mode voltage in a three-level neutral-point-clamped inverter-based induction motor drive for pump and fan applications. Chen et al. [94] performed a comparative study based on both experimental measurements and theoretical analysis on a 2.1kW induction machine. It is showed that the soft switching inverter did not assist in bearing currents mitigation compared to an equivalent hard switched converter. De Broe et al. [95] developed a space vector PWM control strategy for a full controlled rectifier and inverter combination to reduce the common mode neutral-to-ground voltage magnitude in induction machines from V_{dc} to $2V_{dc}/3$. However, it requires a fully controlled rectifier,

and hence is not suitable for drives fed with a diode rectifier. Moreover, the switching frequency must be synchronous between the rectifier and inverter, which is challenging to achieve in practice without compromising other aspects of performance.

A single-phase, multi-level, half-bridge inverter with opposite polarity to the main 3 phase inverter was used as active common mode voltage compensator in [96]. An additional 4th leg was introduced into a traditional 3 phase inverter along with a four phase LC filter in [97]. By appropriate modulation strategies, this configuration can eliminate the common mode voltage while outputting a sinusoidal line-to-line voltage. Von Jouanne et al. [98] proposed a dual-bridge inverter that was found to virtually eliminate the shaft voltage and bearing currents. Additionally, it significantly reduced the leakage current with an appropriate modulation strategy. However, it must be used in combination with a dual-voltage motor operating at the lower voltage rating. The system complexity increases as a result of the additional 3 bridges, which adds the cost of 6 more IGBTs. Tekwani et al. [99] proposed a dual five-level inverter topology and switching strategy to eliminate the common mode voltage for open ended winding induction machines. Chandrashekar et al. [100] concluded that the common mode voltage, shaft voltage and bearing current of 3-level inverters are lower than equivalent 2-level converter. Furthermore, Sunitha et al. [101] note that a multi-level inverter generates lower v_b and i_b than a 3-level converter due to the reduction of dv/dt and increase of rise time. Further examples of modulation techniques can be found in [102] and [125] while a variety of novel converter topologies can be found in [126] and [154].

In summary, for conventional 3 phase 2-level inverters, the space vector can be selected to minimize the common mode voltage, but it cannot be eliminated completely by this approach. In order to eliminate the common mode voltage, new topologies with additional circuit elements are necessary. These new topologies include the 4th leg or the dual inverter to cancel the common mode voltage in the opposing polarity, cascade multi-level inverters to reduce the dv/dt, auxiliary circuits in the DC bus to actively control the DC voltage (i.e., reducing the common mode voltage amplitude). These inverter side mitigation methods act directly on the source so that they are effective for all four bearing current mechanisms.

B. MITIGATION ON THE CONNECTION

This subsection presents a review of mitigation methods applied to the connections between the machine and its associated inverter. These methods include passive/active filters, common mode chokes and shielded cables.

Passive filters, reactors and sinusoidal filters all act to reduce the dv/dt of the motor terminals. Employing filters can result in the reduction of ground current and circulating current for 30%-50%, as demonstrated to experimentally in [17]. As the filters do not eliminate the common mode voltage, the EDM current is more of less unaffected [17]. Additional examples of studies investigation the role of filters can be found in [155] and [183]. An active common-noise canceler (ACC) fed from the DC bus and fed into the connecting wires was designed by Ogasawara et al. [184], [185] to efficiently reduce conducted EMI as well as motor shaft voltage and bearing current.

The common mode choke at the inverter output is able to suppress the common mode current as suggested in [186]. Hence the ground current as well as the circulating current can be reduced. The EDM current remains unaffected as the common mode choke does not modify the common mode voltage.

The use of shielded cables can reduce the ground impedance between stator to ground, resulting in a reduction in the rotor ground current. On the other hand, it increases the stator ground current, which can lead to an increase in the circulating bearing current. This approach does not have any influence on the EDM current [17], [187].

C. MITIGATION IN THE MOTOR

Modifications on the motor can be carried out at design stage or following installation. Bearing current can be suppressed by increasing the magnitude of the impedance or reduced the electromagnetic coupling between winding, stator, and rotor.

Insulated bearings or coated bearings have been a long-standing and effective means of suppressing the low frequency "classic" bearing currents. With a discrete polymer sleeve or aluminum oxide layer on the outer races, additional resistance and capacitance is introduced into the bearing current path. In this way, all various bearing current mechanisms are reduced. The use of hybrid bearings with ceramic balls can also suppress entirely all types of bearing currents. However, hybrid bearings tend to be more expensive than the insulated bearings [17].

An electrostatic shielded induction motor (ESIM) was proposed in [188]. This motor was capable of reducing the shaft voltages below the bearing lubricant breakdown threshold. The insertion of a Faraday shield into the airgap can attenuate the electric field coupling between stator and rotor whereas its insertion in the slot can eliminate the electric coupling between windings and stator. This can suppress the bearing currents. Further electrostatic shield designs can be found in [189] and [193].

As the design stage, the motor can be modified to reduce the bearing currents with only marginal influence on its performance. Oblique slots can be incorporated with a view to reducing the winding-to-rotor capacitance, in turn reducing the BVR and hence reducing the bearing currents without affecting the machine performance. This approach has been investigated using 2D FEM but not experimentally [194]. If the slot fill factor is relatively low, there is space for re-arranging the winding configuration to reduce the winding-to-rotor capacitance [58]. Other machine design modifications can be found in literature, including inter-alia, insulated rotor [195, 196], adding capacitors between the brackets and the stator core [197], adding capacitors between

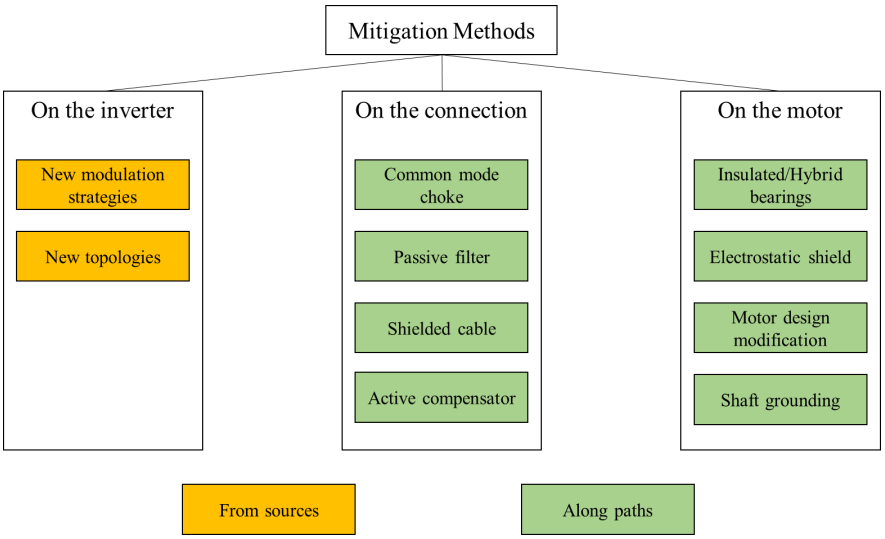

FIGURE 19. Categorization of main mitigation methods on bearing currents.

brackets and the neutral line of the inverter dc link [198], optimizing the magnetic flux-path in BLDC [52] and insulating circular comb-like coil in the stator slots [199].

Conducting brushes can be used to connect the shaft and the frame, creating a short circuit path in parallel with the bearings to limit the bearing voltage and hence prevent bearing breakdown. However, the brushes require periodic maintenance and occasional replacement. The use of multiple conductive microfibers to bridge the bearings using the electrical field emission effect was proposed in [27]. This acts as a mean of bypassing the bearings. This allows the bearing voltage to discharge while also delivering ultra-low friction. This solution, which was detailed in [28], proved effective in suppressing the EDM current.

D. SUMMARY

In this subsection, a summary of mitigation methods has been presented. Fig. 19 categories these methods based on their application: on the inverter, on the connection, on the motor.

Improved modulation strategies and new topologies of inverters reduce the amplitude of the common mode voltage and/or reduce the dv/dt. They are considered to reduce the bearing currents from the perspective of the source.

Other mitigation methods are implemented along the various conduction paths either by increasing the impedance of the bearing current loop or by providing a low impedance path for the induced current to bypass the bearings.

TABLE 2 presents a summary of comparison of merits and drawbacks of various mitigation methods. As indicated in TABLE 2, mitigation methods are not all effective for reduction of all the types of bearing current. Some methods could even lead to increment of certain type of bearing currents. This requires an understanding of bearing current mechanism before the selection of appropriate mitigation methods. Most mitigation methods come with additional cost, which again requires high accuracy modelling of bearing current to determine necessity of implementing the mitigation.

VIII. DISCUSSION AND FUTURE PERSPECTIVES

In literature, existing high frequency bearing current models solve the EDM and circulating bearing current components separately [22], [23]. These approaches are based on an arguably unproven assumption that the electric field and magnetic field behavior can be fully decoupled. Furthermore, these do not consider the nonlinearity of soft magnetic materials. Relatively few published studies have quantified the two bearing current components simultaneously [69], [76]. However, even in these cases, the windings were modelled as a single homogenous region, neglecting the turn-to-turn capacitance and mutual inductance, without accounting for magnetic saturation effect on high frequency eddy-currents in the stator and rotor laminations. The drawbacks of linearized representations can be illustrated by considering the classical skin depth equation and the magnetization curve of a typical stator core material (M270-35A). If the material non-linearity is not accounted for by adopting a single relative permeability of 700 at 1.5T [200], the skin depth is underestimated by 58% compared to the calculation which uses the relative permeability of 123 at 1.8T [200]. Thus, the corresponding resistance and inductance are overestimated by 138%. In machine cores, the flux densities vary spatially, in time, and with fundamental load current. Hence, using the permeability at an a-priori fixed flux density for skin depth and impedance can lead to significant error.

Based on the above discussion, future perspectives on bearing currents modelling may include:

- Build a detailed winding model which includes end-winding, turn-to-turn capacitance, and turn-to-frame capacitance;
- Consider the uneven distribution of voltage stress between turns, hence the different contribution of each turn to the total common mode current;
- Develop a uniform model that can predict all bearing current types simultaneously;

TABLE 2. Comparison of Mitigation Methods.

Mitigation methods	Effectiveness	Merits	Drawbacks
A hybrid selective harmonic elimination PWM scheme with filter [93]	-Effective for all four bearing current mechanisms	-Effectively control the CMV at both low frequency and high frequency	-Only tested for fan or pump applications
A space vector PWM control strategy for a fully controlled rectifier and inverter [95]	-Effective for all four bearing current mechanisms	-The CMV of a typical PWM rectifier/inverter can be markedly reduced	-Need fully controlled rectifier
A single-phase, multi-level, half-bridge inverter with opposite polarity [96]	-Effective for all four bearing current mechanisms	-The bearing current can be reduced by 98.6%	-Additional hardware
An additional 4th leg with LC filter [97]	-Effective for all four bearing current mechanisms	-Completely eliminates the CMV	-Additional hardware
A dual-bridge inverter [98]	-Effective for all four bearing current mechanisms	-Can eliminate the shaft voltage and bearing currents and significantly reduce the leakage current	-Add the cost of 6 more IGBTs -Need dual 3-phase machine
A dual five-level inverter topology and switching strategy [99]	-Effective for all four bearing current mechanisms	-Completely eliminate the common-mode voltages	-Complex system
Passive filters, reactors and sinusoidal filters [17]; The common mode choke [186]	-Ground current and circulating current reduced -EDM current unaffected	-Simple structure	-Suppression of the common mode current, but not the common mode voltage -Each application requires calibration
An active common-noise canceler [184, 185]	-Efficiently reduce conducted EMI as well as motor shaft voltage and bearing current	-Significantly reduce ground current, EMI and shaft voltage	-Additional hardware and a more complex control
Shielded cables [17, 187]	-Reduction in the rotor ground current. Increment of the stator ground current and the circulating bearing current -EDM current unaffected	-Reduce EMI and voltage reflection	-Possible increment of circulating bearing currents
Hybrid bearings with ceramic balls [17]	-Effective for all four bearing current mechanisms	-Simple structure	-More expensive bearings
An electrostatic shielded induction motor [188]	-Effective for all four bearing current mechanisms	-The shield's effect on electrostatic coupling is significant and nearly complete	-Need sufficient air gap to insert the Faraday shield
Multiple conductive microfibers [28]	-Effective for all four bearing current mechanisms	-Good electrical contact -Low friction	-Additional costs
Oblique slots [194]	-Effective for EDM current	-It can reduce the shaft-to-frame voltage by 98%	-Compromise the machine's electromagnetic performances

- Consider the non-linearity saturation of stator and rotor core caused by fundamental current and its influence on the bearing currents;
- Include the effects of the connection cables into the bearing current model.

After an accurate modelling of bearing currents with a inverter-cable-machine system, the bearing breakdown and lifetime may be evaluated, which includes:

- A solid understanding of bearing breakdown: fluid dynamics to depict the lubricant oil film, molecular ionization process at microscopic level, and statistics description of bearing behaviors at macroscopic level;
- Lifetime and maintenance cycle prediction;
- Online condition monitoring of bearing operation.

For the applications which requires high reliability or have difficulty to replace the bearings, proper mitigation methods should be selected carefully with a balance of effectiveness/reliability and additional cost/complexity. Possible works in the mitigation includes:

- Novel modulation technologies of multi-phase or multi-level inverters to reduce CMV;
- Novel machine designs to reduce the high frequency coupling but maintain the same level of electromagnetic performance;
- Low-cost components to insulate or bypass the bearings.

IX. CONCLUSION

In this paper, the mechanisms of the different types of bearing currents in VFDs are introduced in detail. It is demonstrated that the common mode voltage generated by PWM switching is the fundamental source of the high frequency bearing currents.

Even through the causes of bearing currents are clearly demonstrated in literature, the modelling of AC machines in high frequency and prediction of bearing currents is far from straightforward. A range of modelling and parameter identification methods have been introduced and compared, including curve fitting of measured data, analytical calculations, and 2D/3D FEM. Continually improving the accuracy of models while maintaining a competitive level of computational efficiency is challenging. This review has demonstrated that advances still need to be made in models which can accurately calculate the capacitive EDM current as well as the inductive circulating current. Some of the factors that need to be accounted for are end winding effects, turn-to-turn capacitance, skin and proximity effects in stator and rotor lamination.

ACKNOWLEDGMENT

This work was supported by the U.K. Engineering and Physical Sciences Research Council (EPSRC) under Research Award EP/W015838/1. For the purpose of open access, the authors have applied a Creative Commons Attribution (CC BY) license to any Author Accepted Manuscript version arising.

REFERENCES

[1] P. L. Alger and H. W. Samson, "Shaft currents in electric machines," *Trans. Amer. Inst. Electr. Engineers*, vol. 43, pp. 235–245, Jan. 1924.
[2] I. Kerszenbaum, "Shaft currents in electric machines fed by solid-state drives," in *Proc. IEEE Conf. Rec. Ind. Commercial Power Syst. Tech. Conf.*, May 1992, pp. 71–79.
[3] M. J. Costello, "Shaft voltages and rotating machinery," *IEEE Trans. Ind. Appl.*, vol. 29, no. 2, pp. 419–426, Mar. 1993.
[4] D. Macdonald and W. Gray, "A practical guide to understanding bearing damage related to PWM drives," in *Proc. Conf. Rec. Annu. Pulp Paper Ind. Tech. Conf.*, Jun. 1998, pp. 159–165.
[5] M. Bjekic, D. Stojanovic, M. Rosic, and M. Bozic, "Analysis of mitigation techniques for bearing currents in PWM inverter drives," *Metalurgia Int.*, vol. 18, no. 2, pp. 91–97, 2013.
[6] A. von Jouanne, H. Zhang, and A. K. Wallace, "An evaluation of mitigation techniques for bearing currents, EMI and overvoltages in ASD applications," *IEEE Trans. Ind. Appl.*, vol. 34, no. 5, pp. 1113–1122, Sep. 1998.
[7] L. Yang, S. Wang, and J. Feng, "Electromagnetic interference modeling and suppression techniques in variable-frequency drive systems," *Frontiers Mech. Eng.*, vol. 13, no. 3, pp. 329–353, Sep. 2018.
[8] T. Hadden, J. W. Jiang, B. Bilgin, Y. Yang, A. Sathyan, H. Dadkhah, and A. Emadi, "A review of shaft voltages and bearing currents in EV and HEV motors," in *Proc. 42nd Annu. Conf. IEEE Ind. Electron. Soc.*, Oct. 2016, pp. 1578–1583.
[9] T. Plazenet, T. Boileau, C. Caironi, and B. Nahid-Mobarakeh, "An overview of shaft voltages and bearing currents in rotating machines," in *Proc. IEEE Ind. Appl. Soc. Annu. Meeting*, Oct. 2016, pp. 1–8.
[10] S. Chen, T. A. Lipo, and D. Fitzgerald, "Source of induction motor bearing currents caused by PWM inverters," *IEEE Trans. Energy Convers.*, vol. 11, no. 1, pp. 25–32, Mar. 1996.
[11] S. Chen, T. A. Lipo, and D. Fitzgerald, "Modeling of motor bearing currents in PWM inverter drives," *IEEE Trans. Ind. Appl.*, vol. 32, no. 6, pp. 1365–1370, Nov. 1996.
[12] T. G. Arora, M. M. Renge, and M. V. Aware, "Effects of switching frequency and motor speed on common mode voltage, common mode current and shaft voltage in PWM inverter-fed induction motors," in *Proc. 12th IEEE Conf. Ind. Electron. Appl. (ICIEA)*, Jun. 2017, pp. 583–588.
[13] F. Wang, "Motor shaft voltages and bearing currents and their reduction in multilevel medium-voltage PWM voltage-source-inverter drive applications," *IEEE Trans. Ind. Appl.*, vol. 36, no. 5, pp. 1336–1341, Sep./Oct. 2000.
[14] W. Hofmann and J. Zitzelsberger, "PWM-control methods for common mode voltage minimization—A survey," in *Proc. Int. Symp. Power Electron., Electr. Drives, Autom. Motion*, May 2006, pp. 1162–1167.
[15] A. Muetze, "Bearing currents in inverter-fed AC-motors," Ph.D. dissertation, Dept. Elect. Eng. Inf. Technol., Darmstadt Univ. Technol., Darmstadt, Germany, 2004.
[16] A. Muetze, "On a new type of inverter-induced bearing current in large drives with one journal bearing," *IEEE Trans. Ind. Appl.*, vol. 46, no. 1, pp. 240–248, Jan. 2010.
[17] A. Muetze and A. Binder, "Experimental evaluation of mitigation techniques for bearing currents in inverter-supplied drive-systems—Investigations on induction motors up to 500 kW," in *Proc. IEEE Int. Electric Mach. Drives Conf.*, Jun. 2003, pp. 189–186.
[18] A. Muetze and A. Binder, "Calculation of circulating bearing currents in machines of inverter-based drive systems," in *Proc. Conf. Rec. IEEE Ind. Appl. Conf., 39th IAS Annu. Meeting*, Oct. 2004, pp. 720–726.
[19] A. Muetze and A. Binder, "Systematic approach to bearing current evaluation in variable speed drive systems," *Eur. Trans. Electr. Power*, vol. 15, no. 3, pp. 217–227, 2005.
[20] A. Muetze and A. Binder, "Don't lose your bearings," *IEEE Ind. Appl. Mag.*, vol. 12, no. 4, pp. 22–31, Jul. 2006.
[21] A. Muetze and A. Binder, "Calculation of influence of insulated bearings and insulated inner bearing seats on circulating bearing currents in machines of inverter-based drive systems," *IEEE Trans. Ind. Appl.*, vol. 42, no. 4, pp. 965–972, Jul. 2006.
[22] A. Muetze and A. Binder, "Calculation of circulating bearing currents in machines of inverter-based drive systems," *IEEE Trans. Ind. Electron.*, vol. 54, no. 2, pp. 932–938, Apr. 2007.
[23] A. Muetze and A. Binder, "Calculation of motor capacitances for prediction of the voltage across the bearings in machines of inverter-based drive systems," *IEEE Trans. Ind. Appl.*, vol. 43, no. 3, pp. 665–672, May 2007.

[24] A. Muetze, A. Binder, H. Vogel, and J. Hering, "Experimental evaluation of the endangerment of ball bearings due to inverter-induced bearing currents," in *Proc. Conf. Rec. IEEE Ind. Appl. Conf., 39th IAS Annu. Meeting.*, Oct. 2004, pp. 1989–1995.

[25] A. Muetze, A. Binder, H. Vogel, and J. Hering, "What can bearings bear?" *IEEE Ind. Appl. Mag.*, vol. 12, no. 6, pp. 57–64, Nov. 2006.

[26] A. Muetze, V. Niskanen, and J. Ahola, "On radio-frequency-based detection of high-frequency circulating bearing current flow," *IEEE Trans. Ind. Appl.*, vol. 50, no. 4, pp. 2592–2601, Jul. 2014.

[27] A. Muetze and H. W. Oh, "Application of static charge dissipation to mitigate electric discharge bearing currents," *IEEE Trans. Ind. Appl.*, vol. 44, no. 1, pp. 135–143, Jan. 2008.

[28] A. Muetze and H. W. Oh, "Current-carrying characteristics of conductive microfiber electrical contact for high frequencies and current amplitudes: Theory and applications," *IEEE Trans. Power Electron.*, vol. 25, no. 8, pp. 2082–2092, Aug. 2010.

[29] A. Muetze and E. G. Strangas, "On inverter induced bearing currents, bearing maintenance scheduling, and prognosis," in *Proc. Int. Conf. Electr. Mach. (ICEM)*, Sep. 2014, pp. 1915–1921.

[30] A. Muetze and E. G. Strangas, "The useful life of inverter-based drive bearings: Methods and research directions from localized maintenace to prognosis," *IEEE Ind. Appl. Mag.*, vol. 22, no. 4, pp. 63–73, Jul. 2016.

[31] A. Muetze, J. Tamminen, and J. Ahola, "Influence of motor operating parameters on discharge bearing current activity," in *Proc. IEEE Energy Convers. Congr. Expo.*, Sep. 2010, pp. 2739–2746.

[32] A. Muetze, J. Tamminen, and J. Ahola, "Influence of motor operating parameters on discharge bearing current activity," *IEEE Trans. Ind. Appl.*, vol. 47, no. 4, pp. 1767–1777, Jul./Aug. 2011.

[33] S. Chen, *Bearing Current, EMI and Soft Switching in Induction Motor Drives: A Systematic Analysis, Design and Evaluation*. Madison, WI, USA: Univ. of Wisconsin-Madison, Department of Electrical and Computer Engineering, 1995.

[34] S. Chen and T. A. Lipo, "Circulating type motor bearing current in inverter drives," *IEEE Ind. Appl. Mag.*, vol. 4, no. 1, pp. 32–38, Jan. 1998.

[35] D. Dahl, D. Sosnowski, D. Schlegel, R. J. Kerkman, and M. Pennings, "Field experience identifying electrically induced bearing failures," in *Proc. Conf. Rec. Annu. Pulp Paper Ind. Tech. Conf.*, Jun. 2007, pp. 155–163.

[36] P. Mäki-Ontto, "Modeling and reduction of shaft voltages in AC motors fed by frequency converters," Ph.D. dissertation, Dept. Elect. Commun. Eng., Helsinki Univ. Technol., Helsinki, Finland, 2006.

[37] A. F. Moreira, T. A. Lipo, G. Venkataramanan, and S. Bernet, "High-frequency modeling for cable and induction motor overvoltage studies in long cable drives," *IEEE Trans. Ind. Appl.*, vol. 38, no. 5, pp. 1297–1306, Sep. 2002.

[38] N. Idir, Y. Weens, M. Moreau, and J. J. Franchaud, "High-frequency behavior models of AC motors," *IEEE Trans. Magn.*, vol. 45, no. 1, pp. 133–138, Jan. 2009.

[39] H. De Paula, D. A. de Andrade, M. L. R. Chaves, J. L. Domingos, and M. A. A. de Freitas, "Methodology for cable modeling and simulation for high-frequency phenomena studies in PWM motor drives," *IEEE Trans. Power Electron.*, vol. 23, no. 2, pp. 744–752, Mar. 2008.

[40] R. Naik, T. A. Nondahl, M. J. Melfi, R. Schiferl, and J.-S. Wang, "Distributed parameter circuit model for shaft voltage prediction in induction motors fed by PWM based AC drives," in *Proc. Conf. Rec. IEEE Ind. Appl. Conf., 36th IAS Annu. Meeting*, May 2001, pp. 1118–1122.

[41] R. Naik, T. A. Nondahl, M. J. Melfi, R. Schiferl, and J.-S. Wang, "Circuit model for shaft voltage prediction in induction motors fed by PWM-based AC drives," *IEEE Trans. Ind. Appl.*, vol. 39, no. 5, pp. 1294–1299, Sep. 2003.

[42] G. Vidmar and D. Miljavec, "A universal high-frequency three-phase electric-motor model suitable for the delta- and star-winding connections," *IEEE Trans. Power Electron.*, vol. 30, no. 8, pp. 4365–4376, Aug. 2015.

[43] O. Magdun and A. Binder, "High-frequency induction machine modeling for common mode current and bearing voltage calculation," *IEEE Trans. Ind. Appl.*, vol. 50, no. 3, pp. 1780–1790, May/Jun. 2014.

[44] A. Boglietti, A. Cavagnino, and M. Lazzari, "Experimental high-frequency parameter identification of AC electrical motors," *IEEE Trans. Ind. Appl.*, vol. 43, no. 1, pp. 23–29, Jan. 2007.

[45] K. Jia, G. Bohlin, M. Enohnyaket, and R. Thottappillil, "Modelling an AC motor with high accuracy in a wide frequency range," *Electr. Power Appl., IET*, vol. 7, no. 2, pp. 116–122, Feb. 2013.

[46] K. Ito, Y. Sato, T. Zanma, S. Doki, and M. Ishida, "Identification of the parameters of the high-frequency equivalent circuit of PM synchronous motor based on genetic algorithm," *Electr. Eng. Jpn.*, vol. 167, no. 4, pp. 57–66, Jun. 2009.

[47] J. M. Erdman, R. J. Kerkman, D. W. Schlegel, and G. L. Skibinski, "Effect of PWM inverters on AC motor bearing currents and shaft voltages," *IEEE Trans. Ind. Appl.*, vol. 32, no. 2, pp. 250–259, Mar. 1996.

[48] D. Busse, J. Erdman, R. J. Kerkman, D. Schlegel, and G. Skibinski, "Bearing currents and their relationship to PWM drives," *IEEE Trans. Power Electron.*, vol. 12, no. 2, pp. 243–252, Mar. 1997.

[49] D. Busse, J. Erdman, R. J. Kerkman, D. Schlegel, and G. Skibinski, "System electrical parameters and their effects on bearing currents," *IEEE Trans. Ind. Appl.*, vol. 33, no. 2, pp. 577–584, Mar. 1997.

[50] B. Mirafzal, G. L. Skibinski, R. M. Tallam, D. W. Schlegel, and R. A. Lukaszewski, "Universal induction motor model with low-to-high frequency-response characteristics," *IEEE Trans. Ind. Appl.*, vol. 43, no. 5, pp. 1233–1246, Sep. 2007.

[51] J. Adabi, F. Zare, A. Ghosh, and R. D. Lorenz, "Calculations of capacitive couplings in induction generators to analyse shaft voltage," *IET Power Electron.*, vol. 3, no. 3, p. 379, 2010.

[52] K.-T. Kim and J. Hur, "Optimization of magnetic flux-path design for reduction of shaft voltage in IPM-type BLDC motor," *J. Electr. Eng. Technol.*, vol. 9, no. 6, pp. 2187–2193, Nov. 2014.

[53] Y. Wang, B. Bai, and W. F. Liu, "Research on discharging bearing currents of PWM inverter-fed variable frequency induction motor," in *Proc. 17th Int. Conf. Electr. Mach. Syst. (ICEMS)*, Oct. 2014, pp. 1–6.

[54] Y. Wang, W. Liu, Z. Chen, and B. Bai, "Calculation of high frequency bearing currents of PWM inverter-fed VF induction motor," in *Proc. Int. Power Electron. Appl. Conf. Exp.*, Nov. 2014, pp. 1428–1433.

[55] M. Mechlinski, S. Schroder, J. Shen, and R. W. De Doncker, "Common-mode voltage limits for the transformerless design of MV drives to prevent bearing current issues," in *Proc. IEEE Energy Convers. Congr. Expo. (ECCE)*, Sep. 2016, pp. 1–5.

[56] J.-K. Park, T. R. Wellawatta, Z. Ullah, and J. Hur, "New equivalent circuit of the IPM-Type BLDC motor for calculation of shaft voltage by considering electric and magnetic fields," *IEEE Trans. Ind. Appl.*, vol. 52, no. 5, pp. 3763–3771, Sep./Oct. 2016.

[57] T. Svimonishvili, F. Fan, K. Y. See, X. Liu, M. A. Zagrodnik, and A. K. Gupta, "High-frequency model and simulation for the investigation of bearing current in inverter-driven induction machines," in *Proc. IEEE Region 10 Conf. (TENCON)*, Nov. 2016, pp. 55–59.

[58] J.-K. Park, T. R. Wellawatta, S.-J. Choi, and J. Hur, "Mitigation method of the shaft voltage according to parasitic capacitance of the PMSM," *IEEE Trans. Ind. Appl.*, vol. 53, no. 5, pp. 4441–4449, Sep./Oct. 2017.

[59] M. Schuster, J. Springer, and A. Binder, "Comparison of a 1.1 kW-induction machine and a 1.5 kW-PMSM regarding common-mode bearing currents," in *Proc. Int. Symp. Power Electron., Electr. Drives, Autom. Motion (SPEEDAM)*, Jun. 2018, pp. 1–6.

[60] M. T. A. Êvo and H. Paula, "Electrostatic shielding for bearings discharge currents attenuation: Analysis of its effectiveness, losses and impact on the motor performance—A study for design guidelines," *IET Electr. Power Appl.*, vol. 14, no. 6, pp. 1050–1059, 2020.

[61] Y. Liu, J. Cao, Y. Song, G. Xu, and L. Li, "Research on bearing current detection method of high-speed motor driven by PWM inverter," in *Proc. 22nd Int. Conf. Electr. Mach. Syst. (ICEMS)*, Aug. 2019, pp. 1–6.

[62] V. Kindl, B. Skala, R. Pechanek, M. Byrtus, and K. Hruska, "Calculation of induction machine parasitic capacitances using finite element method," in *Proc. ELEKTRO*, May 2016, pp. 176–179.

[63] O. A. Mohammed, S. Ganu, N. Abed, S. Liu, and Z. Liu, "High frequency PM synchronous motor model determined by FE analysis," *IEEE Trans. Magn.*, vol. 42, no. 4, pp. 1291–1294, Apr. 2006.

[64] C. S. Chaves, J. R. Camacho, H. de Paula, M. L. R. Chaves, and E. Saraiva, "Capacitances calculation using FEM for transient overvoltage and common mode currents prediction in inverter-driven induction motors," in *Proc. IEEE Trondheim PowerTech*, Jun. 2011, pp. 1–7.

[65] Z. Li, X. Ma, K. Dong, W. Shen, and W. Zhao, "Study and discussion on the problems of shaft voltage and bearing current in wind power generation system," in *Proc. 9th IEEE Conf. Ind. Electron. Appl.*, Jun. 2014, pp. 1696–1700.

[66] R. Liu, X. Ma, X. Ren, J. Cao, and S. Niu, "Comparative analysis of bearing current in wind turbine generators," *Energies*, vol. 11, no. 5, p. 1305, May 2018.

[67] J. Li, R. Liu, B. Zheng, Y. Zhang, and I. I. A. Soc, "The effects of end part of winding on parasitic capacitances of induction motor fed by PWM inverter," in *Proc. 15th Int. Conf. Elect. Mach. Syst.*, Oct. 2012, pp. 1–5.
[68] C. Jaeger, I. Grinbaum, and J. Smajic, "Numerical simulation and measurement of common-mode and circulating bearing currents," in *Proc. 22nd Int. Conf. Electr. Mach. (ICEM)*, Sep. 2016, pp. 486–491.
[69] A. Bubert, J. Zhang, and R. W. De Doncker, "Modeling and measurement of capacitive and inductive bearing current in electrical machines," in *Proc. Brazilian Power Electron. Conf. (COBEP)*, Nov. 2017, pp. 1–6.
[70] P. Maki-Ontto, H. Kinnunen, and J. Luomi, "Three-phase model for the circuit simulation of common-mode phenomena and shaft voltages in AC motor drive systems," in *Proc. IEEE Int. Conf. Electr. Mach. Drives*, May 2005, pp. 437–443.
[71] P. Maeki-Ontto and J. Luomi, "Common mode flux calculation of AC machines," in *Proc. 15th Int. Conf. Electr. Mach. Drives (ICEM)*, 2002, pp. 1–15.
[72] P. Mäki-Ontto and J. Luomi, "Circumferential flux as a source of bearing current of converter-fed AC machines," in *Proc. NORPIE*, 2002, pp. 12–14.
[73] P. Maki-Ontto and J. Luomi, "Induction motor model for the analysis of capacitive and induced shaft voltages," in *Proc. IEEE Int. Conf. Electr. Mach. Drives*, May 2005, pp. 1653–1660.
[74] O. Magdun, Y. Gemeinder, and A. Binder, "Rotor impedance of the high frequency circulating bearing current path in inverter-fed AC machines," in *Proc. IEEE Energy Convers. Congr. Expo.*, Sep. 2013, pp. 3512–3519.
[75] A. Bobon, P. Zientek, R. Niestroj, M. Pasko, and J. Kwak, "The computational and measurement methods of research on factors affecting the flow of bearing currents in high power induction motors," in *Proc. 13th Sel. Issues Electr. Eng. Electron. (WZEE)*, May 2016, pp. 1–6.
[76] M. Jaritz, C. Jaeger, M. Bucher, J. Smajic, D. Vukovic, and S. Blume, "An improved model for circulating bearing currents in inverter-fed AC machines," in *Proc. IEEE Int. Conf. Ind. Technol. (ICIT)*, Feb. 2019, pp. 225–230.
[77] D. F. Busse, J. M. Erdman, R. J. Kerkman, D. W. Schlegel, and G. L. Skibinski, "The effects of PWM voltage source inverters on the mechanical performance of rolling bearings," *IEEE Trans. Ind. Appl.*, vol. 33, no. 2, pp. 567–576, Mar. 1997.
[78] J. Adabi, F. Zare, G. Ledwich, and A. Ghosh, "Leakage current and common mode voltage issues in modern AC drive systems," in *Proc. Australas. Universities Power Eng. Conf.*, Dec. 2007, pp. 476–481.
[79] Y. Gemeinder, M. Schuster, B. Radnai, B. Sauer, and A. Binder, "Calculation and validation of a bearing impedance model for ball bearings and the influence on EDM-currents," in *Proc. Int. Conf. Electr. Mach. (ICEM)*, Sep. 2014, pp. 1804–1810.
[80] O. Magdun and A. Binder, "Calculation of roller and ball bearing capacitances and prediction of EDM currents," in *Proc. 35th Annu. Conf. IEEE Ind. Electron.*, Nov. 2009, pp. 1051–1056.
[81] J.-H. Jun, C.-K. Lee, and B.-I. Kwon, "The analysis of bearing current using common mode equivalent circuit parameters by FEM," in *Proc. Int. Conf. Electr. Mach. Syst.*, Sep. 2005, pp. 49–51.
[82] J. Adabi, F. Zare, G. Ledwich, A. Ghosh, and R. D. Lorenz, "Bearing damage analysis by calculation of capacitive coupling between inner and outer races of a ball bearing," in *Proc. 13th Int. Power Electron. Motion Control Conf.*, Sep. 2008, pp. 903–907.
[83] Z. Cay, O. Henze, and T. Weiland, "Modeling and simulation of rolling element bearings in inverter-fed AC motors," in *Proc. Int. Symp. Power Electron., Electr. Drives, Autom. Motion*, Jun. 2008, pp. 1333–1336.
[84] H. Prashad, "Effect of operating parameters on the threshold voltages and impedance response of non-insulated rolling element bearings under the action of electrical currents," *Wear*, vol. 117, no. 2, pp. 223–240, Jun. 1987.
[85] X. Zhu, N. Shi, Y. Li, Y. Yang, and X. Wang, "Bearing capacitance estimation of electric vehicle driving motor," *IOP Conf. Ser., Earth Environ. Sci.*, vol. 199, Dec. 2018, Art. no. 032065.
[86] Z. Krzemien, "Phenomena appearing in oil film of bearings in induction motors supplied from PWM inverters," in *Proc. 5th Int. Conf. Electr. Mach. Syst.*, Aug. 2001, pp. 293–296.
[87] X. Ren, R. Liu, and E. Yang, "Modelling of the bearing breakdown resistance in bearing currents problem of AC motors," *Energies*, vol. 12, no. 6, p. 1121, Mar. 2019.
[88] A. Kempski, R. Strzelecki, R. Smolenski, and Z. Fedyczak, "Bearing current path and pulse rate in PWM-inverter-fed induction," in *Proc. IEEE 32nd Annu. Power Electron. Spec. Conf.*, Jun. 2001, pp. 2025–2030.
[89] A. Kempski, "Capacitively coupled discharging currents in bearings of induction motor fed from PWM (pulsewidth modulation) inverters," *J. Electrostatics*, vols. 51–52, pp. 416–423, May 2001.
[90] X. Shancheng and W. Zhengguo, "Characteristic research of bearing currents in inverter-motor drive systems," in *Proc. 5th Int. Power Electron. Motion Control Conf.*, Aug. 2006, pp. 1–4.
[91] R. F. Schiferl and M. J. Melfi, "Bearing current remediation options," *IEEE Ind. Appl. Mag.*, vol. 10, no. 4, pp. 40–50, Jul. 2004.
[92] K. R. M. N. Ratnayake and Y. Murai, "A novel PWM scheme to eliminate common-mode voltage in three-level voltage source inverter," in *Proc. Rec., 29th Annu. IEEE Power Electron. Spec. Conf.*, May 1998, pp. 269–274.
[93] Z. Zhao, Y. Zhong, H. Gao, L. Yuan, and T. Lu, "Hybrid selective harmonic elimination PWM for common-mode voltage reduction in three-level neutral-point-clamped inverters for variable speed induction drives," *IEEE Trans. Ind. Electron.*, vol. 27, no. 3, pp. 1152–1158, Mar. 2012.
[94] S. Chen and T. A. Lipo, "Bearing currents and shaft voltages of an induction motor under hard- and soft-switching inverter excitation," *IEEE Trans. Ind. Appl.*, vol. 34, no. 5, pp. 1042–1048, Sep. 1998.
[95] A. M. De Broe, A. L. Julian, and T. A. Lipo, "Neutral-to-ground voltage minimization in a PWM-rectifier/inverter configuration," *Electr. Mach. Power Syst.*, vol. 26, no. 7, pp. 741–748, Aug. 1998.
[96] Y. Q. Xiang, "A novel active Common-mode-voltage compensator (ACCom) for bearing current reduction of PWM VSI-fed induction motors," in *Proc. 13th Annu. Appl. Power Electron. Conf. Expo.*, Feb. 1998, pp. 1003–1009.
[97] A. L. Julian, G. Oriti, and T. A. Lipo, "Elimination of common-mode voltage in three-phase sinusoidal power converters," *IEEE Trans. Power Electron.*, vol. 14, no. 5, pp. 982–989, Sep. 1999.
[98] A. von Jauanne and H. Zhang, "A dual-bridge inverter approach to eliminating common-mode voltages and bearing and leakage currents," *IEEE Trans. Power Electron.*, vol. 14, no. 1, pp. 43–48, Jan. 1999.
[99] P. N. Tekwani, R. S. Kanchan, K. Gopakumar, and A. Vezzini, "A five-level inverter topology with common-mode voltage elimination for induction motor drives," in *Proc. Eur. Conf. Power Electron. Appl.*, Sep. 2005, pp. 1–10.
[100] S. M. Chandrashekar, A. Ramachandran, and M. C. Reddy, "Simulation and experimental measurement of shaft voltage, bearing current in induction motor drive," in *Proc. IEEE Int. Conf. Power, Control, Signals Instrum. Eng. (ICPCSI)*, Sep. 2017, pp. 732–737.
[101] P. M. Sunitha, B. Banakara, and S. Reddy, "Modeling, simulation and analysis of common mode voltage, bearing voltage and bearing current in PWM multilevel inverter fed induction motor with long cable," in *Proc. 2nd IEEE Int. Conf. Recent Trends Electron., Inf. Commun. Technol. (RTEICT)*, May 2017, pp. 1161–1167.
[102] H. A. Hussain and H. A. Toliyat, "Reduction of shaft voltages and bearing currents in five-phase induction motors," in *Proc. IEEE Energy Convers. Congr. Expo. (ECCE)*, Sep. 2012, pp. 3309–3316.
[103] L.-H. Kim, N.-K. Hahm, C.-Y. Won, K.-H. Han, and Y.-R. Kim, "A new PWM method for conducted EMI reduction in inverter fed motor drive," in *Proc. 20th Annu. IEEE Appl. Power Electron. Conf. Expo.*, Mar. 2005, pp. 1871–1876.
[104] J. Zitzelsberger and W. Hofmann, "Effects of modified modulation strategies on bearing currents and operational characteristics of AC induction machines," in *Proc. 30th Annu. Conf. IEEE Ind. Electron. Soc.*, Nov. 2004, pp. 3025–3030.
[105] N. L. H. Bang, N. V. Nho, N. K. T. Tam, and N. M. Dung, "A phase shifted PWM technique for common-mode voltage reduction in five level H-bridge cascaded inverter," in *Proc. Int. Conf. Utility Exhib. Green Energy Sustain. Develop.*, Mar. 2014, pp. 1–7.
[106] P. S. Behera, G. Vivek, and M. Barai, "Common mode voltage (CMV) in three level NPC VSI using advanced bus clamping methods: A study," in *Proc. Int. Conf. Recent Innov. Electr., Electron. Commun. Eng. (ICRIEECE)*, Jul. 2018, pp. 895–900.
[107] X. Guo, D. Xu, and B. Wu, "Common-mode voltage mitigation for back-to-back current-source converter with optimal space-vector modulation," *IEEE Trans. Power Electron.*, vol. 31, no. 1, pp. 688–697, Jan. 2016.
[108] R. K. Gupta, A. Somani, K. K. Mohapatra, and N. Mohan, "Space vector PWM for a direct matrix converter based open-end winding AC drives with enhanced capabilities," in *Proc. 25th Annu. IEEE Appl. Power Electron. Conf. Expo. (APEC)*, Feb. 2010, pp. 901–908.

[109] A. Iqbal, R. Alammari, M. Mosa, and H. Abu-Rub, "Finite set model predictive current control with reduced and constant common mode voltage for a five-phase voltage source inverter," in *Proc. IEEE 23rd Int. Symp. Ind. Electron. (ISIE)*, Jun. 2014, pp. 479–484.
[110] A. Janabi and B. Wang, "Hybrid space vector pulse width modulation synthesis to minimize the common-mode voltage," in *Proc. IEEE Appl. Power Electron. Conf. Expo. (APEC)*, Mar. 2018, pp. 872–879.
[111] A. Janabi and B. Wang, "Hybrid SVPWM scheme to minimize the common-mode voltage frequency and amplitude in voltage source inverter drives," *IEEE Trans. Power Electron.*, vol. 34, no. 2, pp. 1595–1610, Feb. 2019.
[112] J. Liu, Q. Ge, X. Wang, and L. Tan, "Common-mode voltage reduction method for three-level NPC converter," in *Proc. Int. Conf. Electr. Mach. Syst. (ICEMS)*, Oct. 2013, pp. 1826–1829.
[113] P. Khoa-Dang and N. Nho-Van, "Pulse-width modulation strategy for common mode voltage elimination with reduced common mode voltage spikes in multilevel inverters with extension to over-modulation mode," *J. Power Electron.*, vol. 19, no. 3, pp. 727–743, May 2019.
[114] H.-P. Le-Nguyen and N.-V. Nguyen, "A novel carrier based PWM technique with common-mode voltage reduction for rotor side converter in doubly-fed induction generator," in *Proc. Int. Elect. Eng. Congr. (iEECON)*, Mar. 2018, pp. 1–7.
[115] U. R. Muduli and R. K. Behera, "Constant switching frequency DTC SVPWM with reduced common mode voltage for two level five phase induction motor drives," in *Proc. IEEE Int. Conf. Power Electron., Drives Energy Syst. (PEDES)*, Dec. 2018, pp. 1–6.
[116] N. Rashidirad, E. Afjei, and A. Jalali, "A novel modulation method in a four-level inverter to eliminate bearing currents," in *Proc. 22nd Iranian Conf. Electr. Eng. (ICEE)*, May 2014, pp. 533–538.
[117] J. Shang and Y. W. Li, "A reduced common-mode voltage space vector modulation method for current source converters," in *Proc. 28th Annu. IEEE Appl. Power Electron. Conf. Expo. (APEC)*, Mar. 2013, pp. 394–401.
[118] J. Shang and Y. W. Li, "A space-vector modulation method for common-mode voltage reduction in current-source converters," *IEEE Trans. Power Electron.*, vol. 29, no. 1, pp. 374–385, Jan. 2014.
[119] J. Shang, Y. W. Li, N. R. Zargari, and Z. Cheng, "PWM strategies for common-mode voltage reduction in current source drives," *IEEE Trans. Power Electron.*, vol. 29, no. 10, pp. 5431–5445, Oct. 2014.
[120] Z. Wang, "Reduction of common mode voltage of 2-level voltage source inverter-fed machine," in *Proc. Asian Conf. Energy, Power Transp. Electrific.*, 2017, pp. 1–5.
[121] R. K. Gupta, K. K. Mohapatra, and N. Mohan, "Open-end winding AC drives with enhanced reactive power support to the grid while eliminating switching common-mode voltage," in *Proc. 35th Annu. Conf. IEEE Ind. Electron.*, Nov. 2009, pp. 700–707.
[122] A. Virtanen, M. Jussila, and H. Tuusa, "Comparison of common-mode voltages in frequency converters with alternative space vector modulation methods," in *Proc. IEEE Power Electron. Spec. Conf.*, Jun. 2008, pp. 2248–2256.
[123] M. Fernandez, A. Sierra-Gonzalez, E. Robles, I. Kortabarria, E. Ibarra, and J. L. Martin, "New modulation technique to mitigate common mode voltage effects in star-connected five-phase AC drives," *Energies*, vol. 13, no. 3, p. 607, Jan. 2020.
[124] H. Gao, B. Wu, D. Xu, M. Pande, and R. P. Aguilera, "Common-mode-voltage-reduced model-predictive control scheme for current-source-converter-fed induction motor drives," *IEEE Trans. Power Electron.*, vol. 32, no. 6, pp. 4891–4904, Jun. 2017.
[125] G. Mondal, F. Sheron, A. Das, K. Sivakumar, and K. Gopakumar, "A DC-link capacitor voltage balancing with CMV elimination using only the switching state redundancies for a reduced switch count multilevel inverter fed IM drive," *EPE J.*, vol. 19, no. 1, pp. 5–15, Mar. 2009.
[126] C. Bharatiraja, J. L. Munda, S. Raghu, T. R. Chelliah, and M. Tariq, "Design and implementation of fourth arm for elimination of bearing current in NPC-MLI fed induction motor drive," in *Proc. IEEE Int. Conf. Power Electron., Drives Energy Syst. (PEDES)*, Dec. 2016, pp. 1–6.
[127] D. Ronanki and P. Perumal, "A SVPWM for reduction in common mode and bearing currents applied to diode clamped three-level inverter fed induction motor," in *Proc. IEEE Int. Power Electron. Motion Control Conf. (PEMC)*, Sep. 2016, pp. 1170–1175.
[128] S. De Caro, S. Foti, T. Scimone, A. Testa, G. Scelba, M. Pulvirenti, and S. Russo, "Over-voltage mitigation on SiC based motor drives through an open end winding configuration," in *Proc. IEEE Energy Convers. Congr. Expo. (ECCE)*, Oct. 2017, pp. 4332–4337.
[129] D. Barater, G. Franceschini, F. Immovilli, and E. Lorenzani, "Investigation on H-8 VSI architecture for bearing currents mitigation in VFD," in *Proc. 43rd Annu. Conf. IEEE Ind. Electron. Soc.*, Oct. 2017, pp. 4391–4396.
[130] A. S. Abdel-Khalik, A. Elserougi, A. M. Massoud, and S. Ahmed, "A cascaded boost inverter-based open-end winding three-phase induction motor drive for photovoltaic-powered pumping applications," in *Proc. 4th Int. Conf. Electr. Power Energy Convers. Syst. (EPECS)*, Nov. 2015, pp. 1–6.
[131] M. Aresteh, A. Rahmati, S. Farhangi, and A. Abrishamifar, "Bearing current reduction in a five level flying capacitor DTC drive," *Przeglad Elektrotechniczny*, vol. 87, no. 4, pp. 286–292, 2011.
[132] C. Bharatiraja, R. Selvaraj, T. R. Chelliah, J. L. Munda, M. Tariq, and A. I. Maswood, "Design and implementation of fourth arm for elimination of bearing current in NPC-MLI-fed induction motor drive," *IEEE Trans. Ind. Appl.*, vol. 54, no. 1, pp. 745–754, Jan. 2018.
[133] G. Shiny and M. R. Baiju, "Three-level inverter scheme with common-mode voltage elimination for an open-end winding induction motor drive," in *Proc. IEEE Int. Conf. Power Electron., Drives Energy Syst. (PEDES)*, Dec. 2016, pp. 1–6.
[134] G. S. Chandini, G. Shiny, and M. R. Baiju, "Common-mode voltage eliminated 2-level PWM inverter based on a cascaded 3-level inverter," in *Proc. Int. Conf. Electr., Electron., Optim. Techn. (ICEEOT)*, Mar. 2016, pp. 561–566.
[135] R. K. Dhatrak, R. K. Nema, S. K. Dash, and D. M. Deshpande, "Mitigation of bearing current and shaft voltage using five level inverter in three phase induction motor drive with SPWM technique," in *Proc. Int. Conf. Ind. Instrum. Control (ICIC)*, May 2015, pp. 1184–1189.
[136] R. K. Gupta, K. K. Mohapatra, A. Somani, and N. Mohan, "Direct-matrix-converter-based drive for a three-phase open-end-winding AC machine with advanced features," *IEEE Trans. Ind. Electron.*, vol. 57, no. 12, pp. 4032–4042, Dec. 2010.
[137] D. Han, W. Lee, S. Li, and B. Sarlioglu, "New method for common mode voltage cancellation in motor drives: Concept, realization, and asymmetry influence," *IEEE Trans. Power Electron.*, vol. 33, no. 2, pp. 1188–1201, Feb. 2018.
[138] D. Han, S. Li, W. Lee, and B. Sarlioglu, "Achieving zero common mode voltage generation in a balanced inverter with neutral-point diode-clamping," in *Proc. IEEE Energy Convers. Congr. Expo. (ECCE)*, Oct. 2017, pp. 4351–4357.
[139] D. Han, C. T. Morris, and B. Sarlioglu, "Common-mode voltage cancellation in PWM motor drives with balanced inverter topology," *IEEE Trans. Ind. Electron.*, vol. 64, no. 4, pp. 2683–2688, Apr. 2017.
[140] D. Han, Y. Wu, S. Li, and B. Sarlioglu, "Zero state common mode voltage control in motor drives through inverter topology," in *Proc. IEEE Transp. Electrific. Conf. Expo (ITEC)*, Jun. 2017, pp. 556–560.
[141] H. Zhang, A. V. Jouanne, and S. Dai, "A reduced-switch dual-bridge inverter topology for the mitigation of bearing currents, EMI, and DC-link voltage variations," *IEEE Trans. Ind. Appl.*, vol. 37, no. 5, pp. 1365–1372, Sep. 2001.
[142] A. Hota, S. Jain, and V. Agarwal, "A modified T-structured three-level inverter configuration optimized with respect to PWM strategy used for common-mode voltage elimination," *IEEE Trans. Ind. Appl.*, vol. 53, no. 5, pp. 4779–4787, Sep. 2017.
[143] J. Kalaiselvi and S. Srinivas, "Bearing currents and shaft voltage reduction in dual-inverter-fed open-end winding induction motor with reduced CMV PWM methods," *IEEE Trans. Ind. Electron.*, vol. 62, no. 1, pp. 144–152, Jan. 2015.
[144] H.-P. Krug, T. Kume, and M. Swamy, "Neutral-point clamped three-level general purpose inverter—Features, benefits and applications," in *Proc. IEEE 35th Annu. Power Electron. Spec. Conf.*, Jun. 2004, pp. 323–328.
[145] P. Mäki-Ontto, J. Luomi, and H. Kinnunen, "Reduction of capacitive and induced shaft voltages in an induction motor drive using dual-bridge inverter approach," *Electr. Eng.*, vol. 88, no. 6, pp. 465–472, Aug. 2006.
[146] P. Sandhya, "SVPWM based common mode voltage mitigation using boost converter fed open-end winding AC drive," in *Proc. Int. Conf. Control Commun. Comput. India (ICCC)*, Nov. 2015, pp. 206–211.
[147] K. K. Mohapatra and N. Mohan, "Open-end winding induction motor driven with matrix converter for common-mode elimination," in *Proc. Int. Conf. Power Electron., Drives Energy Syst.*, Dec. 2006, pp. 1–6.
[148] G. Mondal, K. Gopakumar, P. N. Tekwani, and E. Levi, "A multi-level inverter structure with cascaded two-level and three-level inverters for IM drive with CMV elimination and DC-link capacitor voltage balancing," in *Proc. IEEE Ind. Appl. Annu. Meeting*, Sep. 2007, pp. 589–596.

[149] G. Mondal, K. Gopakumar, P. N. Tekwani, and E. Levi, "A five-level inverter scheme with common-mode voltage elimination by cascading conventional two-level and three-level NPC inverters for an induction motor drive," in *Proc. Eur. Conf. Power Electron. Appl.*, Sep. 2007, pp. 1–7.

[150] S. Payami, R. K. Behera, A. Iqbal, and R. A. Al-Ammari, "Common-mode voltage and vibration mitigation of a five-phase three-level NPC inverter-fed induction motor drive system," *IEEE J. Emerg. Sel. Topics Power Electron.*, vol. 3, no. 2, pp. 349–361, Jun. 2015.

[151] B. Li, S. Zhou, D. Xu, S. J. Finney, and B. W. Williams, "A hybrid modular multilevel converter for medium-voltage variable-speed motor drives," *IEEE Trans. Power Electron.*, vol. 32, no. 6, pp. 4619–4630, Jun. 2017.

[152] Y. Xiang, X. Pei, M. Wang, P. Shi, and Y. Kang, "An improved H8 topology for common-mode voltage reduction," *IEEE Trans. Power Electron.*, vol. 34, no. 6, pp. 5352–5361, Jun. 2019.

[153] M. Turzynski and P. J. Chrzan, "Reducing common-mode voltage and bearing currents in quasi-resonant DC-link inverter," *IEEE Trans. Power Electron.*, vol. 35, no. 9, pp. 9553–9562, Sep. 2020.

[154] M. Turzyński and M. Frivaldsky, "Modeling of a quasi-resonant DC link inverter dedicated to common-mode voltage and ground current reduction," *Energies*, vol. 13, no. 19, p. 5090, Sep. 2020.

[155] H. Akagi and S. Tamura, "A Passive EMI filter for eliminating both bearing current and ground leakage current from an inverter-driven motor," *IEEE Trans. Power Electron.*, vol. 21, no. 5, pp. 1459–1469, Sep. 2006.

[156] E. R. Anagha, P. V. Nisha, and T. K. Sindhu, "Design of an active EMI filter for bearing current elimination in VFD," in *Proc. IEEE Int. Symp. Electromagn. Compat. IEEE Asia–Pacific Symp. Electromagn. Compat. (EMC/APEMC)*, May 2018, pp. 131–134.

[157] A. Bhakthavachala, S. T. Kalyani, and K. Anuradha, "A simplified filter topology for compensating common mode voltage and electromagnetic interference in induction motor drives," in *Proc. 1st Int. Conf. Power Eng. Comput. Control*, vol. 117, V. T. Sreedevi, S. Hemamalini, and C. Vaithilingam, Eds., 2017, pp. 377–384.

[158] D. Wen, L. Chuan, J. Jianguo, H. Lipei, and T. Shinzo, "Filter design of restraining over-voltage and bearing current in induction motor fed by PWM inverter," in *Proc. IEEE Region 10 Conf. Comput., Commun., Control Power Eng.*, Oct. 2002, pp. 2083–2086.

[159] M. C. Di Piazza, A. Ragusa, and G. Vitale, "Common mode active filtering effects in induction motor drives for application in electric vehicles," in *Proc. IEEE Vehicle Power Propuls. Conf.*, Sep. 2009, pp. 1421–1427.

[160] M. C. Di Piazza, A. Ragusa, and G. Vitale, "Effects of common-mode active filtering in induction motor drives for electric vehicles," *IEEE Trans. Veh. Technol.*, vol. 59, no. 6, pp. 2664–2673, Jul. 2010.

[161] M. C. Di Piazza, A. Ragusa, and G. Vitale, "Magnetic material performance of transformers in common mode active EMI filters for bearing current suppression," *Przeglad Elektrotechniczny*, vol. 87, no. 6, pp. 198–201, 2011.

[162] M. C. Di Piazza, A. Ragusa, and G. Vitale, "Power-loss evaluation in CM active EMI filters for bearing current suppression," *IEEE Trans. Ind. Electron.*, vol. 58, no. 11, pp. 5142–5153, Nov. 2011.

[163] X. Dianguo, G. Qiang, and W. Wei, "Design of a passive filter to reduce common-mode and differential-mode voltage generated by voltage-source PWM inverter," in *Proc. 32nd Annu. Conf. IEEE Ind. Electron.*, Nov. 2006, pp. 2483–2487.

[164] N. B. Elsayed, M. E. Ibrahim, and M. A. Izzularab, "Mitigation of overvoltages at induction motor terminals fed from an inverter through long cable," in *Proc. 20th Int. Middle East Power Syst. Conf. (MEPCON)*, Dec. 2018, pp. 595–602.

[165] A. Esmaeli, B. Jiang, and L. Sun, "Modeling and suppression of PWM inverter's adverse effects," in *Proc. 1st Int. Symp. Syst. Control Aerosp. Astronaut.*, Jan. 2006, pp. 1–6.

[166] A. Esmaeli, Y. Sun, and L. Sun, "Mitigation of the adverse effects of PWM inverter through active filter technique," in *Proc. 1st Int. Symp. Syst. Control Aerosp. Astronaut.*, Jan. 2006, pp. 1–5.

[167] J. Guzinski, "Sensorless direct torque control of induction motor drive with LC filter," in *Proc. 15th Int. Power Electron. Motion Control Conf. (EPE/PEMC)*, Sep. 2012, pp. 1–8.

[168] Y. Jiang, W. Wu, Y. He, H. S.-H. Chung, and F. Blaabjerg, "New passive filter design method for overvoltage suppression and bearing currents mitigation in a long cable based PWM inverter-fed motor drive system," *IEEE Trans. Power Electron.*, vol. 32, no. 10, pp. 7882–7893, Oct. 2017.

[169] J. Yanshu, X. Dianguo, and C. Xiyou, "Analysis and design of a feed-forward-type active filter to eliminate common-mode voltage generated by a PWM inverter," in *Proc. IEEE 28th Annu. Conf. Ind. Electron. Soc.*, Nov. 2002, pp. 771–775.

[170] J. Kalaiselvi and S. Srinivas, "Passive common mode filter for reducing shaft voltage, ground current, bearing current in dual two level inverter fed open end winding induction motor," in *Proc. Int. Conf. Optim. Electr. Electron. Equip. (OPTIM)*, May 2014, pp. 595–600.

[171] J. Kalaiselvi and S. Srinivas, "Design and development of a single CM filter for bearing current and ground current reduction in a dual two level inverter fed open end winding induction motor drive," in *Proc. IEEE Int. Conf. Power Electron., Drives Energy Syst. (PEDES)*, Dec. 2016, pp. 1–6.

[172] M. Hongfei, X. Dianguo, C. Xiyou, and C. Bo, "A new common-mode sinusoidal inverter output filter," in *Proc. IEEE 33rd Annu. IEEE Power Electron. Spec. Conf.*, Jun. 2002, pp. 858–862.

[173] M. Hongfei, X. Dianguo, C. Xiyou, and C. Bo, "A novel common-mode sinusoidal inverter output filter with variable inductor," in *Proc. Power Convers. Conf.*, Apr. 2002, pp. 710–715.

[174] H. F. Ma, D. G. Xu, and L. J. Miao, "Suppression techniques of common-mode voltage generated by voltage source PWM inverter," in *Proc. 4th Int. Power Electron. Motion Control Conf.*, vols. 1–3, 2004, pp. 1533–1538.

[175] P. Pairodamonchai, S. Suwankawin, and S. Sangwongwanich, "Design and implementation of a hybrid output EMI filter for high-frequency common-mode voltage compensation in PWM inverters," *IEEE Trans. Ind. Appl.*, vol. 45, no. 5, pp. 1647–1659, Sep./Oct. 2009.

[176] G. Qiang and X. Dianguo, "A new approach to mitigate CM and DM voltage dv/dt value in PWM inverter drive motor systems," in *Proc. 22nd Annu. IEEE Appl. Power Electron. Conf. Expo.*, Feb. 2007, pp. 1–5.

[177] M. S. Moghaddam, M. T. Bina, M. A. Golkar, and S. S. Kojori, "Optimal design of voltage regulators for static excitation system in synchronous generator to reduce shaft-induced voltage," *TURKISH J. Electr. Eng. Comput. Sci.*, vol. 25, pp. 1827–1839, Jan. 2017.

[178] U. T. Shami and H. Akagi, "Experimental discussions on a shaft end-to-end voltage appearing in an inverter-driven motor," *IEEE Trans. Power Electron.*, vol. 24, no. 6, pp. 1532–1540, Jun. 2009.

[179] P. K. Steimer and M. Winkelnkemper, "Transformerless multi-level converter based medium voltage drives," in *Proc. IEEE Energy Convers. Congr. Expo.*, Sep. 2011, pp. 3435–3441.

[180] Y. Sun, A. Esmaeli, and L. Sun, "A new method to mitigate the adverse effects of PWM inverter," in *Proc. 1st IEEE Conf. Ind. Electron. Appl.*, May 2006, pp. 1–4.

[181] S. Tamura and H. Akagi, "A passive EMI filter with access to the ungrounded motor neutral line-its effect on attenuating bearing current," *Electr. Eng. Jpn.*, vol. 166, no. 2, pp. 78–87, Jan. 2009.

[182] W. Xin, S. Ke, and L. Weiguo, "Design and performance of a passive EMI filter for three-stage aircraft starter/generator system," in *Proc. IEEE Int. Conf. Aircr. Utility Syst. (AUS)*, Oct. 2016, pp. 560–563.

[183] J. Yan-Shu, L. Yu, and Y. Xiao-Yang, "Research on characteristics of common-mode voltage in PWM drive system and its cancellation," in *Proc. 35th Annu. Conf. IEEE Ind. Electron.*, Nov. 2009, pp. 4122–4127.

[184] S. Ogasawara, H. Ayano, and H. Akagi, "An active circuit for cancellation of common-mode voltage generated by a PWM inverter," *IEEE Trans. Power Electron.*, vol. 13, no. 5, pp. 835–841, Sep. 1998.

[185] S. Ogasawara, S. Zhang, and H. Akagi, "Configurations and characteristics of active canceling and compensating circuits for reducing common-mode voltage generated by voltage-source PWM inverters," *Electr. Eng. Jpn.*, vol. 137, no. 1, pp. 57–65, 2001.

[186] C. Mei, J. C. Balda, W. P. Waite, and K. Carr, "Minimization and cancellation of common-mode currents, shaft voltages and bearing currents for induction motor drives," in *Proc. IEEE 34th Annu. Conf. Power Electron. Spec.*, Jun. 2003, pp. 1127–1132.

[187] E. J. Bartolucci and B. H. Finke, "Cable design for PWM variable-speed AC drives," *IEEE Trans. Ind. Appl.*, vol. 37, no. 2, pp. 415–422, Mar. 2001.

[188] D. F. Busse, J. M. Erdman, R. J. Kerkman, D. W. Schlegel, and G. L. Skibinski, "An evaluation of the electrostatic shielded induction motor: A solution for rotor shaft voltage buildup and bearing current," *IEEE Trans. Ind. Appl.*, vol. 33, no. 6, pp. 1563–1570, Nov. 1997.

[189] B. Bai, Y. Wang, and X. Wang, "Suppression for discharging bearing current in variable-frequency motors based on electromagnetic shielding slot wedge," *IEEE Trans. Magn.*, vol. 51, no. 11, pp. 1–4, Nov. 2015.

[190] F. J. T. E. Ferreira, M. V. Cistelecan, and A. T. de Almeida, "Evaluation of slot-embedded partial electrostatic shield for high-frequency bearing current mitigation in inverter-fed induction motors," *IEEE Trans. Energy Convers.*, vol. 27, no. 2, pp. 382–390, Jun. 2012.
[191] S. Gerber and R.-J. Wangi, "Reduction of inverter-induced shaft voltages using electrostatic shielding," in *Proc. Southern Afr. Universities Power Eng. Conf./Robot. Mechatronics/Pattern Recognit. Assoc. South Afr. (SAUPEC/RobMech/PRASA)*, Jan. 2019, pp. 310–315.
[192] R. Liu, E. Yang, J. Chen, and S. Niu, "Novel bearing current suppression approach in doubly-fed induction generators," *IEEE Access*, vol. 7, pp. 171525–171532, 2019.
[193] P. Maki-Ontto and J. Luomi, "Bearing current prevention of converter-fed AC machines with a conductive shielding in stator slots," in *Proc. IEEE Int. Electr. Mach. Drives Conf.*, Jun. 2003, pp. 274–278.
[194] M. Yea and K. J. Han, "Modified slot opening for reducing shaft-to-frame voltage of AC motors," *Energies*, vol. 13, no. 3, p. 760, Feb. 2020.
[195] T. Maetani, Y. Isomura, A. Watanabe, K. Iimori, and S. Morimoto, "Suppressing bearing voltage in an inverter-fed ungrounded brushless DC motor," *IEEE Trans. Ind. Electron.*, vol. 60, no. 11, pp. 4861–4868, Nov. 2013.
[196] T. Maetani, S. Morimoto, K. Iimori, Y. Isomura, and A. Watanabe, "Approaches to suppressing shaft voltage in brushless DC motor driven by PWM inverter," in *Proc. Int. Conf. Electr. Mach. Syst.*, Aug. 2011, pp. 1–6.
[197] Y. Isomura, K. Yamamoto, S. Morimoto, T. Maetani, A. Watanabe, and K. Nakano, "Approaches to suppressing shaft voltage in non-insulated rotor brushless DC motor driven by PWM inverter," in *Proc. Int. Conf. Electr. Mach. Syst. (ICEMS)*, Oct. 2013, pp. 1242–1247.
[198] Y. Isomura, K. Yamamoto, S. Morimoto, T. Maetani, A. Watanabe, and K. Nakano, "Study of the further reduction of shaft voltage of brushless DC motor with insulated rotor driven by PWM inverter," *IEEE Trans. Ind. Appl.*, vol. 50, no. 6, pp. 3738–3743, Nov. 2014.
[199] J.-S. Kim and K.-H. Nam, "A method of lowering bearing current with embedded circular comb-like coil," in *Proc. Conf. Rec. IEEE Ind. Appl. Conf., 35th IAS Annu. Meeting World Conf. Ind. Appl. Electr. Energy*, Oct. 2000, pp. 1670–1674.
[200] *M270-35 Datasheet*, Surahammars Bruks AB, Västmanland, Sweden, 2018.

WENJUN ZHU (Graduate Student Member, IEEE) received the B.Eng. degree in electrical engineering and automation from the Beijing Institute of Technology, Beijing, China, in 2013, the M.S. degree in sustainable energy systems from the University of Edinburgh, Edinburgh, U.K., in 2015, and the M.Eng. degree in electrical engineering from the Beijing Institute of Technology, in 2016. He is currently pursuing the Ph.D. degree with the University of Sheffield.

From 2016 to 2020, he worked in the automotive industry in Shanghai, China. His research interests include modeling and analysis of permanent-magnet machines and motor drive systems.

DANIELE DE GAETANO (Member, IEEE) received the bachelor's degree in electrical engineering from the University of Napoli "Federico II," Napoli, Italy, in 2016, the master's degree in electrical energy engineering from the University of Padova, Padova, Italy, in 2018, and the Ph.D. degree in electrical and electronic engineering from the Power Electronics, Machines, and Control Research Group, University of Nottingham, Nottingham, U.K., in 2022. Currently, he is a Research Associate with the Electronic and Electrical Engineering Department, University of Sheffield, Sheffield, U.K. During his Ph.D., the main research interests include design, modeling, and analysis of multiphase machines and current harmonic injection techniques for industrial and traction applications. His main research interests include analysis, modeling and experimental tests on electrical machine bearing currents.

XIAO CHEN (Senior Member, IEEE) received the B.Eng. and M.Sc. degrees in electrical engineering from the Harbin Institute of Technology, China, in 2009 and 2011, respectively, and the Ph.D. degree in electrical machines from the University of Sheffield, in 2015.

He was a Research Associate at the University of Sheffield, from January 2016 to May 2018, and an Advanced Motor Drive Engineer in Dyson, U.K., from July 2018 to September 2019. Since September 2019, he has been a Lecturer with the Electrical Machines and Drives Group, Department of Electronic and Electrical Engineering, University of Sheffield. His current research interests include high frequency bearing current, manufacturing impact on electrical machine performances, digital twin of electrical machine and drive, and multi-physics modeling of electrical machines.

GERAINT WYN JEWELL received the B.Eng. and Ph.D. degrees in electrical engineering from the University of Sheffield, Sheffield, U.K., in 1988 and 1992, respectively.

Since 1994, he has been a member of Academic Staff with the Department of Electronic and Electrical Engineering, University of Sheffield, where he is currently a Professor of electrical engineering, the Director of the Rolls-Royce University Technology Centre in Advanced Electrical Machines, and the Director of the EPSRC Future Electrical Machines Manufacturing Hub. His current research interests include electrical machines, electro-mechanical actuators, and electromagnetic modeling.

YIHUA HU (Senior Member, IEEE) received the B.S. degree in electrical engineering and the Ph.D. degree in power electronics and drives from the China University of Mining and Technology, in 2003 and 2011, respectively. From 2011 to 2013, he was a Postdoctoral Fellow at the College of Electrical Engineering, Zhejiang University. From 2013 to 2015, he was a Research Associate at the Power Electronics and Motor Drive Group, University of Strathclyde. From 2016 to 2019, he was a Lecturer at the Department of Electrical Engineering and Electronics, University of Liverpool (UoL). Currently, he is a Reader with the Electronics Engineering Department, University of York (UoY). He has published over 120 articles in IEEE TRANSACTIONS journals. His research interests include renewable generation, power electronics converters and control, electric vehicle, more electric ship/aircraft, smart energy systems, and non-destructive test technology. He is a fellow of Institution of Engineering and Technology (FIET). He was awarded the Royal Society Industry Fellowship. He is an Associate Editor of IEEE TRANSACTIONS ON INDUSTRIAL ELECTRONICS, *IET Renewable Power Generation*, *IET Intelligent Transport Systems*, and *Power Electronics and Drives*.